Title of the manuscript:

PUCHI represses early meristem formation in developing lateral roots of *Arabidopsis thaliana*

Authors

Kevin Bellande[1], Duy-Chi Trinh[1, #], Anne-Alicia Gonzalez[2, 3], Emeric Dubois[2, 3], Anne-Sophie Petitot[1], Mikaël Lucas[1], Antony Champion[1], Pascal Gantet[1], Laurent Laplaze[1]*, Soazig Guyomarc'h[1]*

[1] DIADE, Univ Montpellier, IRD, Montpellier, France

[2] Univ Montpellier, CNRS, INSERM, Montpellier France

[3] Montpellier GenomiX, France Génomique, Montpellier, France

[#] Present address: Laboratoire RDP, Université de Lyon 1, ENS-Lyon, CNRS, INRAE, UCBL, 69364 Lyon, France.

* Corresponding authors: Soazig Guyomarc'h and Laurent Laplaze

Email to whom correspondence may be addressed: soazig.guyomarch@ird.fr

Email of all authors: kevin.bellande@ird.fr, duy-chi.trinh@ens-lyon.fr, anne-alicia.gonzalez@mgx.cnrs.fr, emeric.dubois@mgx.cnrs.fr, anne-sophie.petitot@ird.fr, mikael.lucas@ird.fr, antony.champion@ird.fr, pascal.gantet@ird.fr, laurent.laplaze@ird.fr, soazig.guyomarch@ird.fr

Running title: PUCHI represses early lateral root meristem formation

Date of submission: 28 October 2021

Response to reviewers: 3 February 2022

Word count: 5169 words

Number of tables and figures: 5 figures

Supplementary data: 7 supplementary figures, 1 supplementary table

Highlight

Consistent with the hypothesis that mutual inhibition between gene regulatory sub-networks contributes to lateral root formation, we show that *PUCHI* represses early meristematic gene expression in developing root primordia.

Abstract

Lateral root organogenesis is a key process in the development of a plant's root system and its adaptation to the environment. During lateral root formation, an early phase of cell proliferation first produces a four cell-layered primordium and only from this stage onwards is a root meristem-like structure, expressing root stem cell niche marker genes, being established in the developing organ. Previous studies reported that the gene regulatory network controlling lateral root formation is organised into two subnetworks whose mutual inhibition may contribute to organ patterning. *PUCHI* encodes an AP2/ERF-transcription factor expressed early during lateral root primordium development and required for correct lateral root formation. To dissect the molecular events occurring during this early phase, we generated time-series transcriptomic datasets profiling lateral root development in *puchi-1* mutants and wild types. Transcriptomic and reporter analyses revealed that meristem-related genes were expressed ectopically at early stages of lateral root formation in *puchi-1* mutants. We conclude that, consistent with the inhibition of genetic modules contributing to lateral root development, PUCHI represses ectopic establishment of meristematic cell identities at early stages of organ development. These findings shed light on gene network properties that orchestrate correct timing and patterning during lateral root formation.

Keywords

Arabidopsis - Auxin - Cytokinin - Lateral root development - Meristem - Organogenesis - Patterning - PLETHORA - PUCHI

Abbreviations

CHX: cycloheximide

DEGs: differentially expressed genes

DEX: dexamethasone

FRiP: fraction of reads in peaks

GR: glucocorticoid receptor

GO: Gene Ontology

GRN: gene regulatory network

hpg: hours post gravistimulation

LR: lateral root

LRP: lateral root primordium

MS: Murashige and Skoog medium

NAA: 1-naphthalene acetic acid

NPA: N-1-naphthylphthalamic acid

PI: propidium iodide

QC: quiescent centre

RAM: root apical meristem

VLCFA: very long chain fatty acids

WT: wild type

Introduction

Dynamic and plastic development evolved in sessile organisms such as plants to adapt to changing environmental conditions (Morris *et al.*, 2017). Root branching, the production of new lateral roots (LR) from existing roots, is key in elaborating root system architecture (Motte *et al.*, 2019). In the model plant *Arabidopsis thaliana*, LR arise from pre-branch sites originating in the basal meristem close to the root apex (Xuan *et al.*, 2020). Primed pericycle cells at these pre-branch sites enter new rounds of cell divisions producing a lateral root primordium (LRP). The developing LRP, while growing through overlying cell layers, progressively organises into a new root apical meristem (RAM) that ultimately emerges from the parent root and whose activity will determine the later growth of the LR (Malamy *et al.*, 1997; Banda *et al.*, 2019). Remarkably, LRP development is a two-step process featuring an early, so-called morphogenetic phase (stages I to IV) during which cell proliferation generates a four-cell-layered, bulge-shaped LRP and a second, so-called meristematic phase (stages V to VIII) when the LRP further develops to acquire key RAM characteristics (Lucas *et al.*, 2013; Lavenus *et al.*, 2015; Voß *et al.*, 2015; Goh *et al.*, 2016). However, the mechanisms controlling the establishment of a new root meristem and especially, the transition from the early phase of LRP development to the meristematic phase, when key root meristem genes start to be expressed in the centre of the developing LRP, remain unclear.

RAMs are proliferating tissues located at the tip of growing roots within which cell division and differentiation are regulated sequentially. Maintenance of a stem cell niche at the centre of root meristems ensures continuous production of cells and indeterminate organ growth (van den Berg *et al.*, 1995, 1997; Bennett and Scheres, 2010; Trinh *et al.*, 2018). Multiple regulatory components, including transcriptional regulators and hormones, mediate the regulation of cell identity and division activity in RAMs (Himanen *et al.*, 2002; Goh *et al.*, 2012, 2016; Porco *et al.*, 2016; Du and Scheres, 2017, 2018). In *A. thaliana*, networks of key transcription factors including AP2-domain *PLETHORA* (*PLT*), GRAS-family transcription factors *SHORT-ROOT* (*SHR*) and *SCARECROW* (*SCR*), as well as auxin-dependent factors, have been shown to control the patterning of the RAM stem cell niche and specification of its organizing centre, known as the quiescent centre (QC)

(Galinha *et al.*, 2007; Hofhuis *et al.*, 2013; Goh *et al.*, 2016; Du and Scheres, 2017; Shimotohno *et al.*, 2018). Many of these genes are also dynamically expressed during the process of LR formation (Tian *et al.*, 2014; Lavenus *et al.*, 2015; Goh *et al.*, 2016; Du and Scheres, 2017).

Several studies have shown that cell fate acquisition in developing LRP is not dependent on cell lineage but relies on tissue-scale mechanisms and positional signals (Lucas *et al.*, 2013; von Wangenheim *et al.*, 2016). The progressive organisation of the organ could thus result from emerging properties of a complex genetic network possibly integrating chemical and mechanical cues (Banda *et al.*, 2019). Two examples of such patterning mechanisms are the definition of inner and outer domains of the early LRP by the interplay of SHR and SCR expression domains, and the correct patterning of cell divisions at early stages and transition of the developing LRP to the meristematic phase by distinct sets of *PLT* genes (Goh *et al.*, 2016; Du and Scheres, 2017). These data highlight that gene regulatory events during early LRP development are necessary to transition to the second meristem organisation phase.

Inference of the gene regulatory network (GRN) during LR formation suggested that two distinct genetic sub-circuits operate and that their mutual inhibition could be instrumental in LRP developmental patterning (Lavenus *et al.*, 2015). The first one includes genes predominantly expressed in the whole primordium in the early stages, but only in its base in the later phase. The second one includes meristematic genes whose expression initiates during the transition from the morphogenetic phase to the meristematic phase in the tip of the developing primordium, where the new root meristem stem cell niche is established. Mutual inhibition between these two groups of genes may explain the bifurcation between cell identities in the central zone and the flanking domain of the developing LRP (Lavenus *et al.*, 2015). In addition, in complex genetic systems, mutual inhibition motifs associated to positive regulatory cascades can generate sequential waves in gene expression dynamics and control cell state switch over time (Alon, 2007).

PUCHI is an AP2/ERF-family transcription factor belonging to the first GRN sub-circuit and whose loss of function or perturbation in expression kinetics impairs LRP development (Hirota *et al.*, 2007; Kang *et al.*, 2013; Trinh *et al.*, 2019; Toyokura *et al.*, 2019; Goh *et al.*, 2019). GRN inference and

experimental validation previously revealed that PUCHI acted as a master regulator of very long chain fatty acid (VLCFA) biosynthesis during the first phase of LRP development (Trinh *et al.*, 2019). However, the role played by PUCHI-dependent genetic pathways in LRP development remains elusive.

Here, we show that the AP2/ERF-transcription factor PUCHI, which is predominantly expressed at early stages of LR development, controls the correct timing and pattern of expression of transcription factors as well as distribution of hormonal signals that orchestrate meristem formation during late lateral root organogenesis. Root meristem-related genes are ectopically expressed in inner cell layers of early-phase LRP in a *puchi-1* mutant background. Thus, these results support the hypothesis that the inhibition of gene regulatory modules participates in LRP functional patterning, and show that in the absence of PUCHI, the LR gene regulatory network yields premature expression of meristematic genes in inner cells of young LRP.

Materials and Methods

Plant Materials and Constructs, Growth Conditions

A. thaliana plant ecotypes Columbia-0 (Col-0) were used for all experiments and as backgrounds of transgenic lines in this study. *A. thaliana* seeds were surface-sterilized and sown on half strength Murashige and Skoog (½ MS) solid medium with 0.7% (w/v) plant agar supplemented with B5 vitamins. Plates were kept at 4°C for 2 days and then placed in long-day conditions (16-h light/8-h dark cycle) in a vertical position. The *puchi-1* mutant line has previously been described (Hirota *et al.*, 2007). The *promPLT:PLT-YFP* lines were reported in (Galinha *et al.*, 2007; Hofhuis *et al.*, 2013). The *DR5::GFP* synthetic auxin response reporter was described in (Friml *et al.*, 2003), the synthetic cytokinin response reporter *promTCSn::GFP* was described in (Zürcher *et al.*, 2013), and the organising centre markers *QC25::CFP* and *promWOX5::nls:GFP* were described in (ten Hove *et al.*, 2010) and (Goh *et al.*, 2016) respectively.

RNAseq

Col-0 wild type (WT) and *puchi-1* mutant seeds were surface-sterilized and sown on ½ MS solid medium containing 0.7% (w/v) plant agar supplemented with B5 vitamins. Plates were kept at 4°C for 2 days and then placed in continuous light conditions in a vertical position. Gravistimulation were performed on 4-day-old seedlings and root bends were sampled at 12h, 18h, 24h, 30h and 36h after gravistimulation. Three biological replicates (for both Col-0 and *puchi-1*) were used for the RNAseq experiment. For each replicate, root bends of more than 400 seedlings were dissected under a binocular microscope and frozen in liquid nitrogen immediately on harvesting. For reference, approximately 400 mature root segments located between the bend and the shoot were harvested in 4-day-old seedlings at 12h after gravistimulation to be used as a reference of non-gravitropic-stimulated root tissues devoid of developing LRP (termed “No LR” in the data set). Total RNA was extracted using Qiagen RNeasy plant mini kit with an on-column DNAse treatment following the manufacturer’s recommendation (RNAse-free DNAse Set, Qiagen, Crawley, UK). RNA samples were quantified using a Nanodrop ND100 spectrophotometer (Nanodrop, Wilimington, USA) and RNA purity and integrity were evaluated using High-Resolution Automated Electrophoresis 2100 Bioanalyzer system from Agilent Technologies (https://www.agilent.com/en/product/automated-electrophoresis).

RNAseq analyses was performed by the MGX-Montpellier GenomiX platform (https://www.mgx.cnrs.fr/). cDNA libraries were constructed using a Stranded mRNA Prep Ligation kit (Illumina, San Diego, CA, USA) according to the manufacturer’s instructions. Briefly, poly-A RNAs were purified using oligo-d(T) magnetic beads from 310 ng of total RNA. Poly-A RNAs were fragmented and underwent reverse transcription using random hexamers. During the second strand generation step, dUTP substituted dTTP to prevent the second strand being used as a matrix during the final PCR amplification. Double stranded cDNAs were adenylated at their 3' ends and ligated to Illumina's universal anchors. Ligated cDNAs were amplified following 12 PCR cycles. During this PCR, the libraries were indexed, and the adapter’s sequences were completed to be

compatible with the cluster generation step. PCR products were purified using AMPure XP Beads (Beckman Coulter Genomics, Brea, CA, USA). Libraries were validated using a High Sensitivity NGS kit on a Fragment Analyzer (Agilent Technologies, Santa Clara, CA, USA) and quantified using a KAPA Library quantification kit (Roche, Basel, Switzerland).

For library sequencing, 36 libraries were pooled in equimolar amounts. The balance between all samples of the pool was assessed by sequencing on a Miniseq (Illumina, San Diego, CA, USA) using a 300 cycle Mid Output Reagent Cartridge. The pool was then sequenced on a Novaseq 6000 (Illumina, San Diego, CA, USA) S1 flow cell in paired end 2*100 nt mode according to the manufacturer's instructions. This sequencing produced between 36 and 44 million passed filter clusters per library.

For sequencing quality control, image analyses and base calling were performed using the NovaSeq Control Software and Real-Time Analysis component (Illumina, San Diego, CA, USA). Demultiplexing and trimming were performed using Illumina's conversion software (bcl2fastq 2.20). The quality of the raw data was assessed using FastQC from the Babraham Institute and the Illumina software SAV (Sequencing Analysis Viewer). FastqScreen was used to estimate the potential level of contamination.

For alignment and statistical analysis, a splice junction mapper, TopHat 2.1.1 (Kim *et al.*, 2013) (using Bowtie 2.3.5.1 (Langmead *et al.*, 2009)), was used to align the RNA-Seq reads to the *A. thaliana* genome (NCBI TAIR10.1) with a set of gene model annotations (gff file downloaded from NCBI on November 13, 2020). Final read alignments with more than 6 mismatches were discarded. Samtools (v1.9) was used to sort the alignment files. Then, gene counting was performed using Featurecounts 2.0.0 (Liao *et al.*, 2014). As the data is from a strand-specific assay, the reads needed to be mapped to the opposite strand of the gene (-s 2 option). Before statistical analysis, genes with less than 15 reads (cumulating all the analysed samples) were filtered out.

Differentially expressed genes (DEGs) were identified using the Bioconductor (Gentleman *et al.*, 2004) package (http://www.bioconductor.org) DESeq2 1.26.0 (Love *et al.*, 2014) (R version 3.6.1).

Data were normalised using the DESeq2 normalisation method. Genes with an adjusted p-value of less than 5% (according to the False Discovery Rate method by Benjamini-Hochberg) were declared differentially expressed. DEGs between Col-0 and *puchi-1* were then investigated for each time point. The DEGs with a Log2Fold-change ≥1 and a DESeq2 package-Wald Test (*p*-value: p*<0.05; p**<0.02; p***<0.01) were selected for the gene ontology (GO) analysis. GO biological process enrichment analyses of either, the list of up- or down-regulated DEGs in *puchi-1* were performed using a PANTHER Overrepresentation assay (http://pantherdb.org) and Fisher's test followed by a Bonferroni Correction (p*<0.05) (Thomas *et al.*, 2003; Mi *et al.*, 2013). Only the individual elementary annotations of the GO biological process are shown.

RT-qPCR analysis

For RT-qPCR analyses, plant material was collected following the lateral root-induction system described in (Himanen *et al.*, 2002). Briefly, square Petri dishes containing ½ MS solid medium, 0.7% (w/v) plant agar supplemented with B5 vitamins and containing N-1-naphthylphthalamic acid (NPA) and/or 1-naphthalene acetic acid (NAA) were used. Col-0 and *puchi-1* seeds were germinated and grown for 72 h on 5 µM NPA before transfer to 5 µM NPA-containing (control) or 10 µM NAA-containing (lateral root induction) medium. Three biological replicates of root segments without the root apical meristem were harvested after 24h of treatment and immediately frozen in liquid nitrogen for each condition. Total RNA was extracted using a Qiagen RNeasy plant mini kit with an on-column DNAse treatment following the manufacturer's recommended protocol (RNAse-free DNAse Set, Qiagen, Crawley, UK). Quantification, purity and contaminations assessment of the RNA samples were tested using a gel electrophoresis and a Nanodrop ND100 spectrophotometer (Nanodrop, Wilimington, USA). cDNA generated from the three biological replicates were synthetised following the manufacturer's recommended protocol (Omniscript RT Kit, Qiagen, Crawley, UK): 1000 ng of RNA in RNAse free water were heated 10min at 70°C, added to the manufacturer mix (up to 20µL) for 1h at 37°C. Generated cDNA diluted 1/10 were added to the Brilliant III Ultra-Fast SYBR® Green QPCR Master Mix with Low ROX reaction mix

and used to performed qPCR analysis as recommended by the manufacturer (Qiagen, Crawley, UK). All qPCR reactions were carried out and analysed using the Roche® LC480 Lightcycler system and software (qPCR analysis program, Cq determination, curves calibration). Complete thermocycling parameters were as follow: 95°-3'15; 95°-20'', 60°-20'' x 40 cycles; 95°-1', 60°-30'', 95°-30''. Normalisation was achieved with the tubulin *TUB3* gene (AT5G62700) and the *UBQ5* gene (AT3G62250) (Lavenus *et al.*, 2015; Trinh *et al.*, 2019). The calibrator cDNA for relative quantification of the effect of each treatment was the control WT treated with NPA. Data are represented as mean ± SEM (standard error of the means). Significance between NAA treated samples was determined using a Student's t test (p*<0.05; p**<0.02; p***<0.01). The primers used for RT-qPCR analysis were designed to generate 75-110 bases amplicon length. Primer's efficiency and specificity was confirmed by qPCR. Primer sequences were as follows:

AT3G20840: PLT1-F caaccctttcaaacacaagagt; PLT1-R ttggaacctctcctccttca; AT1G51190: PLT2-F aggaaaggaagacaagtctacttagg; PLT2-R agagggaccccaatatttaagtg; AT5G10510: PLT3-F gatctttaccttggaacctttgc; PLT3-R gctgctatgtcatacgcttca; AT5G17430: PLT4/BBM-F gagacaataatagtcactcccgagat; PLT4/BBM-R tttgttcgttattgttaatgttattgc; AT5G57390: PLT5-F ctccatgtacagaggcgtca; PLT5-R gcagcttcctcttgagtgcta; AT5G65510: PLT7-F aacagctgtaggagggaaggt; PLT7-R tctatcttccttgtcatatccaccta; TUB3-F tgcattggtacacaggtgagggaa; TUB3-R agccgttgcatcttggtattgctg; UBQ5-F cgatggatctggaaaggttc; UBQ5-R agctccacaggttgcgttag

Confocal Microscopy, Image Processing and Analysis

Confocal microscopy images were obtained with a LEICA SP8 confocal system using a 40X HCX corr Plan Apochromat CS 1.1 NA water objective. Samples were mounted in water or in 15 µM propidium iodide (PI) for 1-2 h or in 15 µM PI supplemented with 0.004%Triton X-100 for 20-40 min as previously described (Du and Scheres, 2017). All combinatorial fluorescence analyses were run as sequential scans. The following excitation/emission settings were used to obtain specific fluorescence signals: for PI, 488/600 to 620 nm; for YFP, 514/520-550 nm, for CFP, 458/475-505

nm and for EGFP, 488/500 to 550 nm. All post-acquisition image such as channel merging was performed using Fiji (https://imagej.net/Fiji) (Schindelin *et al.*, 2012).

Database mining for PUCHI target genes

Genes showing differential expression (fold change ≥ 1.5, p-value ≤0.05 as determined by Welch two sample t-test) in auxin-treated PUCHI-GR roots upon dexamethasone treatment and in presence of cycloheximide were retrieved from (Trinh *et al.*, 2019). Genes associated to genome sequences bound by the transcription factor PUCHI *in vitro* (ampDAP, FRiP ≥ 5%) were retrieved from the Arabidopsis DAP-seq database published at http://neomorph.salk.edu/dev/pages/shhuang/dap_web/pages/index.php (O'Malley *et al.*, 2016). List contents were compared using the "Calculate and draw custom Venn diagrams" system from VIB / UGent Bioinformatics & Systems (https://bioinformatics.psb.ugent.be/cgi-bin/liste/Venn/calculate_venn) to select genes that had been detected by at least two of the three methods: RNAseq profiling of *puchi-1* roots, DAP-seq using PUCHI as a bait, or inducible complementation of PUCHI-GR *puchi-1* roots. Aliases and description summaries were retrieved for each gene from Thalemine (https://bar.utoronto.ca/thalemine/begin.do). Overrepresentation of Gene Ontologies among the 150 genes that are common between two datasets was assayed using the PANTHER algorithm (http://pantherdb.org) and Fisher's test followed by a Bonferroni Correction (p*<0.05) (Thomas *et al.*, 2003; Mi *et al.*, 2013). Among the list of those 150 genes, transcription factors and genes annotated as related to auxin, cytokinin, VLCFA, LR development, or meristem regulation were selected for closer inspection (see suppl. Table 1 for detailed lists).

Results

Loss of PUCHI function alters sequential expression patterns of *PLETHORA* genes in developing lateral root primordia

To assess the role played by PUCHI in the genetic regulation of LRP development and identify its targets, either direct or indirect, during this organogenesis process, we performed a time-series transcriptomic analysis following LR induction by gravistimulation in Col-0 wild type (WT) and *puchi-1* mutant plants (Fig.1A). Root segments were sampled at 12 hours post gravistimulation (hpg; stage I), 18 hpg (predominantly stage II in Col-0 and *puchi-1*), 24 hpg (stages II-IV in Col-0, stages II-III in *puchi-1*), 30 hpg (stages III-V in Col-0, stages II-IV in *puchi-1*) and 36 hpg (stages III-VI in Col-0, stages II-V in *puchi-1*), which correspond approximately to LR initiation, the mid and late morphogenetic phases, and the early meristematic phase in a Col-0 background in our experimental conditions (Fig. S1A, S1B and S1C) (Goh *et al.*, 2016; Trinh *et al.*, 2019). A root segment was sampled directly upward of the root bend in both genotypes at 12 hpg to be used as "No LR" reference material. RNAseq profiling of these samples was performed and differentially expressed genes (DEGs) between successive time points or between the 2 genotypes at a single time point were identified (Log2FC > 1 or Log2FC < -1, p*<0.05; see Material and methods section).

A total of 5791 genes in WT and 9571 genes in the *puchi-1* mutant background were shown to be differentially expressed during the LRP developmental time course. Noticeably, comparison of WT and *puchi-1* reference "No LR" root segments revealed 361 genes differentially expressed between the two genotypes (Fig. 1B). By contrast, comparison of *puchi-1* to WT LRP transcriptomic datasets at 12, 18, 24, 30, and 36 hpg yielded a minimum of 314 up to a maximum of 1009 DEGs, with the highest divergence between the two genotypes observed at 24 hpg and 36 hpg (Fig.1B). Because we were first interested in uncovering the role of PUCHI in the process of lateral root organogenesis without necessarily distinguishing the primary molecular targets of this transcription factor from the secondary regulatory events influencing LRP formation, we examined all the genes

whose expression dynamics during LRP formation was shown to be dependent on PUCHI function, later termed PUCHI-dependent genes.

We analysed gene ontology (GO) enrichment among differentially expressed genes focusing specifically on genes whose expression is up-regulated in *puchi-1* as compared to WT or on genes whose expression is downregulated in *puchi-1* as compared to WT. Consistent with previous studies, this analysis revealed that PUCHI-dependent genes are highly enriched in lipid metabolism-related genes (*p*-value < 0,001), and confirmed that PUCHI positively influences the expression of multiple VLCFA, cutin, and suberin biosynthetic genes during LRP formation (Fig. 1C-D, Supp. Fig. S2, Supp. Fig. S3) (Trinh *et al.*, 2019). In addition, transcriptomic profiling in *puchi-1* and WT revealed other biological processes dependent on PUCHI. Interestingly, root development related genes were overrepresented in the *puchi-1* RNAseq dataset as compared to WT (p*<0.05 when comparing *puchi-1* and WT at 24h). These genes include *PLT1*, *PLT2*, and *PLT4/BBM* genes, which are well known regulators of root apical meristem establishment and maintenance (Fig. 1D) (Aida *et al.*, 2004). Other genes whose function can be related to root meristem organisation or activity (*e.g.*, predominantly expressed in the QC (Nawy *et al.*, 2005)) displayed altered expression dynamics during LRP development in the *puchi-1* background (Supp. Fig. S3). Especially our RNAseq analysis shows robust overexpression of *PLT1* and *PLT4* genes in *puchi-1* root segments throughout the four time points of our dataset and especially at 18h and 24h, which corresponds to root segments harbouring young LRP from stage II to stage III, *i.e.*, before the transition to the meristematic phase (Fig. 1D, Supp. Fig. S1). Conversely other regulators of the PLETHORA family, *PLT5* and *PLT7,* were downregulated in *puchi-1* root segments as compared to WT (Fig. 1D). These latter results are consistent with previously published LR GRN prediction analyses and confirm that both *PLT5* and *PLT7* genes are positively regulated downstream of *PUCHI* in the early morphogenetic phase (Lavenus *et al.*, 2015). Under expression of *PLT5* and *PLT7* were confirmed by independent RT-qPCR analyses in *puchi-1* roots compared to WT 24h after LR induction by auxin (which correspond to stages II-III LRP in Col-0 and stages I-III LRP in *puchi-1*) (Himanen *et al.*, 2002) (Supp. Fig. S4A).

We took advantage of published *in vitro* and *in vivo* datasets to compare identified DEGs to previously reported PUCHI-dependent gene expression or PUCHI genomic binding sites. First, a list of 13 putative direct target genes of PUCHI were previously identified from the transcriptomic response of PUCHI-GR seedlings' roots upon dexamethasone treatment and in presence of cycloheximide, an inhibitor of protein synthesis (Trinh *et al.*, 2019). Second, a total of 2412 putative PUCHI binding sites have been identified in the genome using the DAP-seq technology (O'Malley *et al.*, 2016). Comparison of those lists to the list of PUCHI-dependent genes identified by RNAseq profiling of branching root segments (this work) yielded 1 single gene, namely *CYTOKININ RESPONSE FACTOR 1* (*CRF1*), that is retrieved by these 3 investigation methods, and a total of 150 genes identified by at least two of these three experimental strategies (Supp. Fig. S5A and Supp. Table 1). Because DAP-seq profiles genomic sequences for which the PUCHI transcription factor displays affinity *in vitro*, and because PUCHI-GR complementation assay was performed in presence of cycloheximide, *CRF1* is most likely a direct target of PUCHI, that induces its expression during LRP formation (Supp. Fig. S3, Supp. Fig. S6E). Interestingly, this gene encodes a component of the cytokinin signalling pathway that modulates a wide range of developmental processes (Raines *et al.*, 2016) (Supp. Fig. S5). Next, a Gene Ontology analysis revealed that genes associated to responses to stresses and to chemical stimuli are overrepresented among the 150 genes shared by at least two of these three experimental datasets (Supp. Table 1). Transcription factor genes and genes associated to auxin and cytokinin homeostasis and signalling pathways, LR development, meristem regulation, and VLCFA biosynthesis are also in this list (Suppl. Fig. S5B and Supp. Table 1). Remarkably, *PLT5*, whose expression dynamics in branching root segments is dependent on PUCHI (this work), was associated to PUCHI-binding sites identified by DAP-seq analysis. Thus, altogether these results suggest that the early expressed LRP regulator PLT5 may also be a direct target gene of PUCHI during lateral root development.

LRP development progression in a *puchi-1* mutant background has previously been shown to be delayed (Hirota *et al.*, 2007; Trinh *et al.*, 2019). To assess the role played by this developmental delay in the transcriptomic gap observed between *puchi-1* and WT LRPs, we analysed the expression profiles of selected genes whose time-dependent expression dynamics during LRP

development have previously been documented (Lavenus *et al.*, 2015; Nagata *et al.*, 2021). In most cases, observed changes in gene expression kinetics between both genotypes were not consistent with, simply, shifted developmental time courses (Supp. Fig. S6 and S7). Taken together, our data confirm that PUCHI activity is required for correct LRP development progression and suggests this transcription factor induces the expression of *CRF1*, *PLT5* and *PLT7* genes and represses the expression of several meristem-specific genes during the LRP early morphogenetic phase.

Meristematic PLT genes are induced prematurely in *puchi-1* LRP

It was previously reported that the transcription factors PLT3, PLT5 and PLT7 control the induction of *PLT1*, *PLT2* and *PLT4* in developing LRP (Du and Scheres, 2017). Unexpectedly, *PLT1* and *PLT4* were overexpressed and *PLT5* and *PLT7* downregulated in *puchi-1* mutant roots, especially in the early stages of development (Fig. 1D; Supp. Fig. S4A). To analyse the impact of *PUCHI* loss of function on the expression pattern of root meristem-related *PLT* genes, transgenic reporter constructs *promPLT1:PLT1-YFP*, *promPLT2:PLT2-YFP*, *promPLT3:PLT3-YFP* and *promPLT4:PLT4-YFP* were introduced into the *puchi-1* mutant background, and their expression pattern compared to that in the WT background (Galinha *et al.*, 2007; Hofhuis *et al.*, 2013). Consistent with our time-course RNAseq results, we observed earlier *PLT1-YFP* and *PLT4-YFP* expression in stages II-III (18h-24h after gravistimulation) in *puchi-1* LRP compared to WT (Fig. 2A-F, 2G-L). Conversely, *PLT3-YFP* expression was weaker in *puchi-1* LRPs, while the PLT2-YFP construct did not display major changes in expression in *puchi-1* compared to WT before LRP emergence (Supp. Fig. S4B-G and H-M). Hence, our results reveal that PUCHI inhibits expression of *PLT1* and *PLT4*, two key root meristem transcription factors, during the early stages of LRP formation.

PUCHI represses expression of QC markers during the early LR development phase

During the first phase of LR organogenesis, anticlinal, periclinal and tangential cell divisions progressively generate a 4-layer LRP that grows against the overlying endodermal layer (Malamy *et al.*, 1997; von Wangenheim *et al.*, 2016). A major developmental transition occurs at this stage, during which the LRP first expresses QC marker genes in inner central cells and acquires a dome shape as it breaks through the endodermis (Lucas *et al.*, 2013; von Wangenheim *et al.*, 2016; Goh *et al.*, 2016). The early expression of meristematic *PLT* genes suggests the transition from the early, morphogenetic to the second, meristematic phase occurred prematurely in the *puchi-1* background. To test this hypothesis and confirm modifications in QC marker gene expressions observed in the RNAseq data (Supp. Fig. S3) (Nawy *et al.*, 2005), we investigated meristem establishment in *puchi-1* LRP using QC marker constructs *QC25::CFP* and *promWOX5::nls:GFP* (ten Hove *et al.*, 2010; Goh *et al.*, 2016). Expression of *QC25::CFP* in Col-0 LRPs was first detected in a few central cells in the second outermost layer from stages IV-V onwards (Fig. 3C, E, G) (Goh *et al.*, 2016; Du and Scheres, 2017). In contrast, in a *puchi-1* loss-of-function background, *QC25::CFP* expression could be detected in young LRPs as early as stage II (Fig. 3B and 3D), and later in a wider domain compared to WT (Fig. 3G-H). Similarly, *promWOX5::nls:GFP* was expressed prematurely in stage II in inner cell layers of *puchi-1* LRPs which correlates with *WOX5* upregulation observed in *puchi-1* RNAseq data as compared to WT at 18 h after LR induction (Fig. 3I-J; Supp. Fig. S3). Furthermore, the *promWOX5::nls:GFP* expression domain stretches to inner cell layers, but also to flanking cells at later stages in *puchi-1* LRPs (Fig. 3K-P). Altogether, our observations show that QC marker gene expression occurs earlier and in a wider domain in *puchi-1* LRPs. We conclude that PUCHI is required to delay the activation of QC marker gene expression during LRP development, possibly *via* repressing *PLT1* and *PLT4* expression at early stages.

Auxin and cytokinin signalling patterns are modified in *puchi* LRP

Auxin distribution regulates *PLT* gene expression and contributes to LRP organisation (Laskowski *et al.*, 2008; Peret *et al.*, 2014; Mähönen *et al.*, 2014; Du and Scheres, 2017; Scheres and Krizek, 2018). Interestingly, our transcriptomic analysis revealed that genes induced by auxin, such as

IAA2, or encoding auxin transporters, such as *PIN1*, *PIN3*, *PIN4* and *PIN7*, were upregulated in the early stages (18 hpg-24 hpg) of LR development in *puchi-1* (Fig. 4A and Supp. Fig. S3) (Bishopp *et al.*, 2011). We used the *DR5::GFP* synthetic auxin response reporter to visualise the pattern of auxin signalling in *puchi-1* LRP compared to WT (Friml *et al.*, 2003). As previously described (Benková *et al.*, 2003), the *DR5::GFP* reporter revealed an auxin response gradient in developing WT LRPs with a maximum close to the LRP tip (Fig. 4B, 4D and 4F). In *puchi-1* mutant LRP too, the *DR5::GFP* reporter signal was non-uniformly distributed and displayed predominant expression in the centre of the primordium in contrast to its flanks (Fig. 4C, 4E and 4G). However, in comparison to the WT situation, *DR5::GFP* expression domain was broader and extended closer to the LRP base in *puchi-1*, especially in primordia from stage IV onwards. Thus, in contrast to previous report based on *DR5::GUS* expression pattern (Hirota *et al.*, 2007), our data suggest that PUCHI is required for the establishment of a WT-like auxin signal gradient during LRP development. We therefore investigated the spatial distribution of PIN1 proteins in Col-0 and *puchi-1* LRP using a *promPIN1:PIN1-GFP* construct (Benková *et al.*, 2003). This revealed PIN1 distribution is strongly impaired in *puchi-1* LRP from stage III onwards, displaying a higher signal in inner cell layers compared to WT (Fig. 4H-O).

Previous studies have shown that cytokinin impacts PIN1 polarization in LRP from stage III onwards by reallocating PIN1 to periclinal membranes (Marhavý *et al.*, 2011, 2014). To test whether *puchi-1* LRP defects are correlated with perturbations in cytokinin signalling patterning, the *promTCSn::GFP* reporter was introduced into the *puchi-1* mutant background and its expression compared to that in WT LRPs (Zürcher *et al.*, 2013). In WT, *promTCSn::GFP* expression was not detected in LRPs before stage VII, and from stage VII onwards the expression of this cytokinin signalling reporter was restricted to pro-vascular cells as previously described (Fig. 4P, 4R and 4T (Bielach *et al.*, 2012). In contrast, *promTCSn::GFP* expression was detected in central cells in the inner layers and extended to flanking regions of *puchi-1* LRP from stage II onwards (Fig. 4Q). In later stages, cytokinin signalling was observed in LRP flanks (Fig. 4S and 4U). We conclude that *PUCHI* loss of function compromises the establishment of auxin and cytokinin response patterns in developing LRPs.

Discussion

Two successive phases were previously described during the process of LR organogenesis before the emergence of a new LR. During the first, so-called morphogenetic phase, cell proliferation generates a four-cell-layered primordium that grows against the overlying endodermis layer. Only at this stage, at about mid-term of the full developmental time course of the LRP, do anatomic features reminiscent of the meristem stem cell niche become apparent in the centre of the primordium, where expression of QC marker genes initiates (Lavenus *et al.*, 2015; Voß *et al.*, 2015; Goh *et al.*, 2016). Onset of QC marker gene expression at this transition stage is dependent on the previous establishment of the layered pattern that is controlled by the SHR/SCR pathway (von Wangenheim *et al.*, 2016; Goh *et al.*, 2016). Next, during the following developmental steps, the root meristem organisation in the centre of the growing primordium becomes more and more complex while surrounding cells retain LRP boundary characteristics (Malamy *et al.*, 1997; Lavenus *et al.*, 2015). After LR emergence, the QC may maintain the indeterminate growth of the LR by repressing differentiation of the surrounding meristematic cells as it is described in primary root meristems (van den Berg *et al.*, 1995). Many transcriptional regulators were shown to be dynamically expressed during the process of LR organogenesis and may participate in the control of cell proliferation and the acquisition of new cell identities. Remarkably, inference of the gene regulatory network controlling LR development suggested that it is organised in two genetic subnetworks whose mutual inhibition may explain LRP development patterning (Lavenus *et al.*, 2015; Voß *et al.*, 2015). One genetic sub-circuit gathers genes, including those encoding the transcription factors ARF7 and PUCHI, that are expressed at early stages in the whole primordium and only in its base in later stages. The second genetic module gathers transcriptional factors such as ARF5 and PLT4 whose expression spans in the central domain of the primordium where the meristem stem cell niche is being established, only in the second phase of its development (Fig. 5).

The transcription factor PUCHI belongs to the former genetic module and is expressed very early in the developing LRP from stage I (Hirota *et al.*, 2007; Trinh *et al.*, 2019; Goh *et al.*, 2019). Interestingly, the correct timing of *PUCHI* induction is essential: the sequential induction of *ARF7*, *LBD16*, and only then *PUCHI*, was shown to be critical for the correct progression of LR formation as premature expression of *PUCHI* disrupted LRP initiation by repressing auxin-induced root branching (Goh *et al.*, 2019). However, how PUCHI function at early stages influences subsequent LRP development remained unclear. Here, we show that meristematic genes, *PLT1* and *PLT4*, as well as root meristem QC marker constructs, *QC25::CFP* and *promWOX5::nls:GFP,* are expressed ectopically at earlier stages and in wider domains in *puchi-1* developing LRP as compared to WT. Conversely *PLT5* and *PLT7*, that belong together with *PUCHI* to the group of genes expressed at early stages of LRP development (Lavenus *et al.*, 2015), are under-expressed in the *puchi-1* loss-of-function background. Although such perturbations are not observed for all the genes in each gene subnetwork, respective changes in *PLT5*, *PLT7*, and root meristem genes expression patterns in *puchi-1* mutant LRPs are consistent with the hypothesis that, at the level of the LR gene regulatory network system, early expressed and root meristematic genes belong to two mutually-exclusive sub-circuits (Lavenus *et al.*, 2015). PUCHI participates in the induction of *PLT5* and *PLT7* expression during lateral root formation, *PLT5* likely being a direct target of the transcription factor PUCHI. It also shows for the first time that PUCHI, which is predominantly expressed at early stages of LRP development, is required for the correct timing of meristem establishment and especially represses premature expression of key meristematic genes at early stages of lateral root development, namely *PLT1*, *PLT4*, and *WOX5*. Remarkably, this is clearly different from the role of PLT3, PLT5 and PLT7 transcription factors which were shown to be required for the correct progression of LRP development and its transition to the meristematic phase (Du and Scheres, 2017). This data points to a complex influence of PUCHI on the gene regulatory network controlling lateral root development, as its control over the expression of its direct target genes may translate into intricate effects on the gene system dynamics.

This raises the question of how PUCHI regulates cell identity acquisition in developing LRPs. Interestingly, cross analysis of three lists of PUCHI-dependent genes highlighted *CRF1* as a likely

direct target gene of PUCHI. This is also supported by *in silico* predictions of PUCHI target genes based on correlated, but delayed, expression profiles (Lavenus *et al.*, 2015). *CRF1* encodes an AP2/ERF transcription factor that, redundantly with other CRFs, mediates part of the cytokinin signalling pathway modulating various plant development processes and responses to abiotic stresses, in interaction with other hormonal signalling pathways (Rashotte *et al.*, 2006). Interestingly, phenotypical analyses of multiple mutant combinations and overexpressing lines revealed complex and redundant influence of CRFs on primary root growth and suggested that at least some members promote lateral root formation (Raines *et al.*, 2016). CRF-dependent expression of PIN-family, auxin transporter genes was shown to contribute to the regulation of primary root growth and lateral root formation by cytokinins (Šimášková *et al.*, 2015). The expression pattern of the cytokinin reporter construct *promTCSn::GFP* and the distribution of the PIN1 reporter PIN1:GFP were shown to be altered in *puchi-1* mutant LRPs as compared to WT (Fig. 4). In the RNAseq profiling of LR development, *CRF1* is the only *CRF* gene displaying such expression dynamics typical of the early expressed subnetwork and positively controlled by PUCHI (Supp. Fig. S3). Thus, *CRF1* may represent a key target of PUCHI impacting the cytokinin and auxin-dependent pathways that regulate LRP organogenesis and patterning.

Interestingly, a number of other transcription factors of the AP2/ERF family were identified as putative PUCHI targets supported by both the RNAseq dataset and the DAP-seq dataset (*PLT5*, *ERF2*, *ERF12*, *ERF53*, *ERF113*, *DDF1*) (Supp. Fig. 5B and Supp. Table 1). Transcription factors of the AP2/ERF family are involved in the regulation of a wide range of developmental processes, in many cases in relation with hormone or stress signalling networks (Horstman *et al.*, 2014; Feng *et al.*, 2020). Interestingly, ERF12 was shown to regulate flower development, possibly by orchestrating the sequential induction and stabilisation of reproductive developmental programs in shoot apices together with PUCHI and related transcription factors (Chandler and Werr, 2020). The expression dynamics of *PLT5* during LR development previously suggested that it was indeed controlled by PUCHI (Lavenus et al., 2005). Redundantly with PLT3 and PLT7, PLT5 was shown to control cell division patterning, correct auxin signal distribution and wild type progression of LRP development including the onset of root meristem gene expression such as *PLT1*, *PLT4* and

WOX5 (Du and Scheres, 2017). Both *PLT5* and *PLT7* expression is downregulated in the *puchi-1* mutant background, and auxin signal distribution and PIN1 localization is also impaired (Fig. 4 and Supp. Fig S3). Expression of *PLT3* and/or modification in expression of PLT5/7-independent genes in *puchi-1* may explain the observed differences between *plt3/5/7* and *puchi-1* LRP phenotypes.

Several genes involved in hormone homeostasis or signalling have also been identified among the PUCHI-dependent genes (Supp. Fig S3, S5B and Supp. Table 1). Auxin and cytokinin are key phytohormones whose roles in functional patterning of meristems and organ primordia have been well described, although in many cases the multiple feedback loops connecting gene regulatory networks and hormonal homeostasis and signalling pathways make any sequential order of molecular events difficult to establish (Chandler and Werr, 2015; Salvi *et al.*, 2020). Here, we show that auxin and cytokinin signalling patterns are impaired in *puchi-1* mutant LRPs. Interestingly, previous reports have shown higher auxin contents in the roots of 5-day-old *puchi-1* seedlings compared to WT (Goh *et al.*, 2019). Alternatively, PUCHI may modulate auxin signalling processes and responses downstream of auxin accumulation, as suggested by the observation that ectopic expression of *PUCHI* in LR founder cells compromises the auxin signal maximum establishment without affecting auxin content (Goh *et al.*, 2019). More specifically, modification of auxin signalling distribution in *puchi-1* mutant LRP correlates with perturbed distribution of PIN1 auxin transporters (Fig. 4A and 4H-O). Formation of an auxin response gradient is critical for proper LRP development (Benková *et al.*, 2003). *PLT1/2/3/4* are well-identified auxin-responsive genes that regulate the establishment and maintenance of a root stem cell niche and this, in turn, regulates the expression and localization of PIN transporters and therefore auxin distribution in the root apical meristem and LRP (Benková *et al.*, 2003; Galinha *et al.*, 2007; Prasad *et al.*, 2011; Pinon *et al.*, 2013; Mähönen *et al.*, 2014; Du and Scheres, 2017).

Cytokinins repress the expression of the PIN auxin efflux carriers in the root meristem and in LRP (Laplaze *et al.*, 2007; Dello Ioio *et al.*, 2008; Růžička *et al.*, 2009; Bishopp *et al.*, 2011). In addition, in the early stages of LRP development, cytokinins modulate PIN1 targeting to periclinal versus anticlinal domains of cell membranes (Marhavý *et al.*, 2011, 2014). Cytokinin signal distribution,

PIN1 expression levels and PIN1-GFP distribution are all modified in *puchi-1* LRPs. As observed for root apical meristem initiation and maintenance, or when an apical root meristem is regenerated after root tip excision, auxin and cytokinin signals define complementary spatial domains that may contribute to the positioning of the new stem cell niche and guide further LRP patterning (Schaller *et al.*, 2015; Efroni *et al.*, 2016). This pattern is not observed in the *puchi-1* background. Altogether, this suggests that compromised auxin and cytokinin response distribution in *puchi-1* LRP may trigger the early ectopic expression of meristematic genes through a PIN1-regulated, auxin-dependent mechanism. Alternatively, misexpression of meristematic genes in *puchi-1* LRP may contribute to disorganize auxin and cytokinin signal distribution and perturb LRP morphogenesis and patterning.

We recently showed that VLCFA biosynthetic enzymes are downstream targets of PUCHI in developing LRP (Trinh *et al.*, 2019). Interestingly, an increasing body of evidence highlights cross-talk between VLCFA and hormones in plant development (Boutté and Jaillais, 2020). For instance, VLCFAs are involved in controlling cell proliferation in shoot organs in a cytokinin-dependent, non-cell autonomous manner (Nobusawa *et al.*, 2013; Boutté and Jaillais, 2020). Furthermore, in the VLCFA mutant *pasticcino1 (pas1)*, the abnormal polar distribution of PIN1 in specific cells results in local alteration of auxin distribution and disturbs LRP formation (Roudier *et al.*, 2010). Last, fused proliferating bulges generated by roots of *puchi* or VLCFA-defective mutants on auxin- and cytokinin-supplemented medium (callus inducing medium), closely resemble that produced by roots of mutants affected in polar auxin transport in response to exogenous auxin supply, as well as those produced by cytokinin-overproducing pericycle upon treatment with a highly diffusible auxin analog (Benková *et al.*, 2003; Geldner *et al.*, 2004; Laplaze *et al.*, 2007; Shang *et al.*, 2016; Trinh *et al.*, 2019). Altogether this data suggests tight links between VLCFA, cytokinin and auxin distribution and LRP patterning. Strikingly, two distinct AP2/ERF-controlled cascades targeting VLCFA biosynthetic enzymes during LRP development were recently described, suggesting that AP2/ERF transcription factors may act as master regulators of VLCFA biosynthesis during LRP formation (Trinh *et al.*, 2019; Guyomarc'h *et al.*, 2021; Lv *et al.*, 2021). Last, VLCFA-containing ceramides were recently shown to participate in a feedforward loop maintaining preferential

584 expression of the transcription factor genes *ATML1 and PDF2*, key regulators of
585 protodermis/epidermis differentiation, in the outer cell layer of developing LRPs (Nagata *et al.*,
586 2021). This function may involve direct binding of these VLCFA-containing ceramides to the
587 START domain of the transcription factors (Nagata *et al.*, 2021). *ATML1* and *PDF2* expression
588 dynamics is lost in *puchi-1* mutant LRP (Supp. Fig S7G-H). Thus, we hypothesise that PUCHI-
589 dependent VLCFA regulation could participate actively in patterning mechanisms controlling LRP
590 organisation.

591 In conclusion, by analysing the impact of *PUCHI* loss of function on the progression of LRP
592 development and functional patterning, we showed that PUCHI is required for the correct timing of
593 meristem establishment and especially, represses premature expression of key root meristem
594 genes at early stages of LRP development. These results are consistent with the model of a LR
595 gene regulatory network organized in distinct genetic sub-circuits whose sequential inhibitions or
596 activations contribute to the transition from an early morphogenetic phase to a second, meristem-
597 establishment phase, as well as to the bifurcation between the central meristematic domain and
598 the flanking domain in the developing organ. How VLCFA-, auxin- or cytokinin-dependent
599 patterning mechanisms may interact during this process downstream of PUCHI will require further
600 investigations.

601

602 **Supplementary data**

603

604 A supplementary figure S1 shows the LRP phenotype in Col-0 and *puchi-1* LRP during the time-
605 course transcriptomic analysis after gravistimulation.

606 A supplementary figure S2 shows the list of all DEGs GO-terms enrichment during the time-course
607 transcriptomic analysis in *puchi-1* compared to Col-0 upon gravistimulation

608 A supplementary figure S3 provides the heat map of selected gene patterns up- and down-
609 regulated in *puchi-1* compared to Col-0 background during the formation of LRP.

A supplementary figure S4 investigates PLTs gene expression analysis in *puchi-1* compared to Col-0 using q-RT PCR and confocal microscopy.

A supplementary figure S5 identified the PUCHI direct target genes using available datasets.

A supplementary figure S6 shows predicted PUCHI target gene expression patterns in *puchi-1* and Col-0 background during the formation of LRP.

A supplementary figure S7 shows selected gene expression patterns in *puchi-1* and Col-0 background during the formation of LRP.

Acknowledgments

We thank Prof. M.J. Bennett for critical reading of the manuscript. We also thank the "Montpellier Ressources Imagerie" imaging facility and Carine Alcon for providing valuable advice for confocal imaging. We thank Julien Lavenus for seminal discussions about this project. This work was supported by the Institute of Research for Development, the University of Montpellier, and the French Agence Nationale de la Recherche through the NewRoot grant (ANR-17-CE13-0004-01). MGX acknowledges financial support from the France Génomique National infrastructure, funded as part of "Investissement d'Avenir" programme at the Agence Nationale de la Recherche (contract ANR-10-INBS-09).

Author contributions

Conceptualisation: L.L., S.G.; Investigation, validation, methodology and formal analysis: K.B., T.-D. C., A.-A. G., E. D., A.-S. P.; Visualization: K.B and S.G.; Writing - original draft: K.B.; Writing - review & editing: K.B., T.D.C., A.-A. G., E. D., M.L., A.C., P.G., L.L., S.G.; Supervision: L.L., S.G.; Funding acquisition: M.L., A.C., P.G., L.L., S.G.

Conflict of interest

The authors declare no conflict of interest.

Funding

This work was supported by the Institute of Research for Development, the University of Montpellier, and the French Agence Nationale de la Recherche through the NewRoot grant (ANR-17-CE13-0004-01). MGX acknowledges financial support from the France Génomique National infrastructure, funded as part of “Investissement d’Avenir” programme at the Agence Nationale de la Recherche (contract ANR-10-INBS-09).

Data availability

All data to support the conclusions of this manuscript are included in the main text and the supplementary materials. The full RNA-seq data discussed in this publication have been deposited in the NCBI's Gene Expression Omnibus and are accessible through GEO Series accession number GSEXXXXXX.

References

Aida M, Beis D, Heidstra R, Willemsen V, Blilou I, Galinha C, Nussaume L, Noh Y-S, Amasino R, Scheres B. 2004. The PLETHORA Genes Mediate Patterning of the Arabidopsis Root Stem Cell Niche. Cell **119**, 109–120.

Alon U. 2007. Network motifs: theory and experimental approaches. Nature Reviews Genetics 2007 8:6 **8**, 450–461.

Banda J, Bellande K, von Wangenheim D, Goh T, Guyomarc'h S, Laplaze L, Bennett MJ. 2019. Lateral Root Formation in Arabidopsis: A Well-Ordered LRexit. Trends in Plant Science **24**, 826–839.

Benková E, Michniewicz M, Sauer M, Teichmann T, Seifertová D, Jürgens G, Friml J. 2003. Local, efflux-dependent auxin gradients as a common module for plant organ formation. Cell **115**, 591–602.

Bennett T, Scheres B. 2010. Root Development—Two Meristems for the Price of One? Current Topics in Developmental Biology **91**, 67–102.

van den Berg C, Willemsen V, Hage W, Weisbeek P, Scheres B. 1995. Cell fate in the Arabidopsis root meristem determined by directional signalling. Nature 1995 378:6552 **378**, 62–65.

van den Berg C, Willemsen V, Hendriks G, Weisbeek P, Scheres B. 1997. Short-range control of cell differentiation in the Arabidopsis root meristem. Nature 1997 390:6657 **390**, 287–289.

Bielach A, Podlešáková K, Marhavý P, Duclercq J, Cuesta C, Müller B, Grunewald W, Tarkowski P, Benková E. 2012. Spatiotemporal Regulation of Lateral Root Organogenesis in *Arabidopsis* by Cytokinin. The Plant Cell **24**, 3967–3981.

Bishopp A, Help H, El-Showk S, Weijers D, Scheres B, Friml J, Benková E, Mähönen AP, Helariutta Y. 2011. A mutually inhibitory interaction between auxin and cytokinin specifies vascular pattern in roots. Current Biology **21**, 917–926.

Boutté Y, Jaillais Y. 2020. Metabolic Cellular Communications: Feedback Mechanisms between Membrane Lipid Homeostasis and Plant Development. Developmental Cell **54**, 171–182.

Chandler JW, Werr W. 2015. Cytokinin–auxin crosstalk in cell type specification. Trends in Plant Science **20**, 291–300.

Chandler JW, Werr W. 2020. A phylogenetically conserved APETALA2/ETHYLENE RESPONSE FACTOR, ERF12, regulates Arabidopsis floral development. Plant Molecular Biology **102**, 39–54.

Du Y, Scheres B. 2017. PLETHORA transcription factors orchestrate de novo organ patterning during Arabidopsis lateral root outgrowth. Proceedings of the National Academy of Sciences of the United States of America **114**, 11709–11714.

Du Y, Scheres B. 2018. Lateral root formation and the multiple roles of auxin. Journal of Experimental Botany **69**, 155–167.

Efroni I, Mello A, Nawy T, Ip PL, Rahni R, Delrose N, Powers A, Satija R, Birnbaum KD. 2016. Root Regeneration Triggers an Embryo-like Sequence Guided by Hormonal Interactions. Cell **165**, 1721–1733.

Feng K, Hou X-L, Xing G-M, Liu J-X, Duan A-Q, Xu Z-S, Li M-Y, Zhuang J, Xiong A-S. 2020. Advances in AP2/ERF super-family transcription factors in plant. Critical Reviews in Biotechnology **40**, 750–776.

Friml J, Vieten A, Sauer M, Weijers D, Schwarz H, Hamann T, Offringa R, Jürgens G. 2003. Efflux-dependent auxin gradients establish the apical-basal axis of Arabidopsis. Nature **426**, 147–153.

Galinha C, Hofhuis H, Luijten M, Willemsen V, Blilou I, Heidstra R, Scheres B. 2007. PLETHORA

proteins as dose-dependent master regulators of Arabidopsis root development. Nature **449**, 1053–1057.

Geldner N, **Richter S**, **Vieten A**, **Marquardt S**, **Torres-Ruiz RA**, **Mayer U**, **Ju□rgens G**. 2004. Partial loss-of-function alleles reveal a role for GNOM in auxin transport-related, post-embryonic development of Arabidopsis. Development **131**, 389–400.

Gentleman RC, Carey VJ, Bates DM, *et al.* 2004. Bioconductor: open software development for computational biology and bioinformatics. Genome Biology **5**, R80.

Goh T, Joi S, Mimura T, Fukaki H. 2012. The establishment of asymmetry in Arabidopsis lateral root founder cells is regulated by LBD16/ASL18 and related LBD/ASL proteins. Development (Cambridge, England) **139**, 883–93.

Goh T, Toyokura K, Wells DM, *et al.* 2016. Quiescent center initiation in the Arabidopsis lateral root primordia is dependent on the SCARECROW transcription factor. Development (Cambridge, England) **143**, 3363–71.

Goh T, Toyokura K, Yamaguchi N, *et al.* 2019. Lateral root initiation requires the sequential induction of transcription factors LBD16 and PUCHI in *Arabidopsis thaliana*. New Phytologist **224**, 749–760.

Guyomarc'h S, Boutté Y, Laplaze L. 2021. AP2/ERF transcription factors orchestrate very long chain fatty acid biosynthesis during Arabidopsis lateral root development. Molecular Plant **14**, 205–207.

Himanen K, Boucheron E, Vanneste S, De Almeida Engler J, Inzé D, Beeckman T. 2002. Auxin-mediated cell cycle activation during early lateral root initiation. Plant Cell **14**, 2339–2351.

Hirota A, Kato T, Fukaki H, Aida M, Tasaka M. 2007. The auxin-regulated AP2/EREBP gene PUCHI is required for morphogenesis in the early lateral root primordium of Arabidopsis. The Plant cell **19**, 2156–68.

Hofhuis H, Laskowski M, Du Y, Prasad K, Grigg S, Pinon V, Scheres B. 2013. Phyllotaxis and rhizotaxis in Arabidopsis are modified by three plethora transcription factors. Current Biology **23**, 956–962.

Horstman A, Willemsen V, Boutilier K, Heidstra R. 2014. AINTEGUMENTA-LIKE proteins: hubs in a plethora of networks. Trends in Plant Science **19**, 146–157.

ten Hove CA, Willemsen V, de Vries WJ, van Dijken A, Scheres B, Heidstra R. 2010. SCHIZORIZA Encodes a Nuclear Factor Regulating Asymmetry of Stem Cell Divisions in the Arabidopsis Root. Current Biology **20**, 452–457.

Dello Ioio R, Nakamura K, Moubayidin L, Perilli S, Taniguchi M, Morita MT, Aoyama T, Costantino P, Sabatini S. 2008. A genetic framework for the control of cell division and differentiation in the root meristem. Science **322**, 1380–1384.

Kang NY, Lee HW, Kim J. 2013. The AP2/EREBP Gene PUCHI Co-Acts with LBD16/ASL18 and LBD18/ASL20 Downstream of ARF7 and ARF19 to Regulate Lateral Root Development in Arabidopsis. Plant and Cell Physiology **54**, 1326–1334.

Kim D, Pertea G, Trapnell C, Pimentel H, Kelley R, Salzberg SL. 2013. TopHat2: accurate alignment of transcriptomes in the presence of insertions, deletions and gene fusions. Genome Biology **14**, R36.

Langmead B, Trapnell C, Pop M, Salzberg SL. 2009. Ultrafast and memory-efficient alignment of short DNA sequences to the human genome. Genome Biology **10**, R25.

Laplaze L, Benkova E, Casimiro I, *et al.* 2007. Cytokinins act directly on lateral root founder cells to inhibit root initiation. The Plant cell **19**, 3889–900.

Laskowski M, Grieneisen VA, Hofhuis H, Hove CA ten, Hogeweg P, Marée AFM, Scheres B. 2008. Root System Architecture from Coupling Cell Shape to Auxin Transport (D Weigel, Ed.). PLoS Biology **6**, e307.

Lavenus J, Goh T, Guyomarc'h S, *et al.* 2015. Inference of the Arabidopsis lateral root gene regulatory network suggests a bifurcation mechanism that defines primordia flanking and central zones. The Plant cell **27**, 1368–88.

Liao Y, Smyth GK, Shi W. 2014. featureCounts: an efficient general purpose program for assigning sequence reads to genomic features. Bioinformatics **30**, 923–930.

Love MI, Huber W, Anders S. 2014. Moderated estimation of fold change and dispersion for RNA-seq data with DESeq2. Genome Biology **15**, 550.

Lucas M, Kenobi K, Wangenheim D von, *et al.* 2013. Lateral root morphogenesis is dependent on the mechanical properties of the overlaying tissues. Proceedings of the National Academy of Sciences **110**, 5229–5234.

Lv B, Wei K, Hu K, *et al.* 2021. MPK14-mediated auxin signaling controls lateral root development via ERF13-regulated very-long-chain fatty acid biosynthesis. Molecular Plant **14**, 285–297.

Mähönen AP, Tusscher K ten, Siligato R, Smetana O, Díaz-Triviño S, Salojärvi J, Wachsman G, Prasad K, Heidstra R, Scheres B. 2014. PLETHORA gradient formation mechanism separates auxin responses. Nature **515**, 125–129.

Malamy JE, Benfey PN, Lanctot A, Feldman TP, Moss BL, Klavins E, Villalobos LIAC, Nemhauser JL. 1997. Organization and cell differentiation in lateral roots of Arabidopsis thaliana. Development (Cambridge, England) **124**, 33–44.

Marhavý P, Bielach A, Abas L, *et al.* 2011. Cytokinin Modulates Endocytic Trafficking of PIN1 Auxin Efflux Carrier to Control Plant Organogenesis. Developmental Cell **21**, 796–804.

Marhavý P, Duclercq J, Weller B, Feraru E, Bielach A, Offringa R, Friml J, Schwechheimer C, Murphy A, Benková E. 2014. Cytokinin controls polarity of PIN1-dependent Auxin transport during lateral root organogenesis. Current Biology **24**, 1031–1037.

Mi H, Muruganujan A, Thomas PD. 2013. PANTHER in 2013: Modeling the evolution of gene function, and other gene attributes, in the context of phylogenetic trees. Nucleic Acids Research **41**, D377–D386.

Morris EC, Griffiths M, Golebiowska A, *et al.* 2017. Shaping 3D Root System Architecture. Current Biology **27**, R919–R930.

Motte H, Vanneste S, Beeckman T. 2019. Molecular and Environmental Regulation of Root Development. Annual Review of Plant Biology **70**, 465–488.

Nagata K, Ishikawa T, Kawai-Yamada M, Takahashi T, Abe M. 2021. Ceramides mediate positional signals in Arabidopsis thaliana protoderm differentiation. Development (Cambridge, England) **148**.

Nawy T, Lee J-Y, Colinas J, Wang JY, Thongrod SC, Malamy JE, Birnbaum K, Benfey PN. 2005. Transcriptional Profile of the Arabidopsis Root Quiescent Center. The Plant Cell **17**, 1908–1925.

Nobusawa T, Okushima Y, Nagata N, Kojima M, Sakakibara H, Umeda M. 2013. Synthesis of Very-Long-Chain Fatty Acids in the Epidermis Controls Plant Organ Growth by Restricting Cell Proliferation (J Chory, Ed.). PLoS Biology **11**, e1001531.

O'Malley RC, Huang S-SC, Song L, Lewsey MG, Bartlett A, Nery JR, Galli M, Gallavotti A, Ecker JR. 2016. Cistrome and Epicistrome Features Shape the Regulatory DNA Landscape. Cell **165**, 1280–1292.

Peret B, Middleton AM, French AP, *et al.* 2014. Sequential induction of auxin efflux and influx carriers regulates lateral root emergence. Molecular Systems Biology **9**, 699–699.

Pinon V, Prasad K, Grigg SP, Sanchez-Perez GF, Scheres B. 2013. Local auxin biosynthesis regulation by PLETHORA transcription factors controls phyllotaxis in Arabidopsis. Proceedings of the National

Academy of Sciences of the United States of America **110**, 1107–12.

Porco S, Larrieu A, Du Y, *et al.* 2016. Lateral root emergence in Arabidopsis is dependent on transcription factor LBD29 regulation of auxin influx carrier LAX3. Development (Cambridge, England) **143**, 3340–9.

Prasad K, Grigg SP, Barkoulas M, *et al.* 2011. Arabidopsis PLETHORA Transcription Factors Control Phyllotaxis. Current Biology **21**, 1123–1128.

Raines T, Shanks C, Cheng C-Y, *et al.* 2016. The cytokinin response factors modulate root and shoot growth and promote leaf senescence in Arabidopsis. The Plant Journal: For Cell and Molecular Biology **85**, 134–147.

Rashotte AM, Mason MG, Hutchison CE, Ferreira FJ, Schaller GE, Kieber JJ. 2006. A subset of Arabidopsis AP2 transcription factors mediates cytokinin responses in concert with a two-component pathway. Proceedings of the National Academy of Sciences of the United States of America **103**, 11081–11085.

Roudier F, Gissot L, Beaudoin F, *et al.* 2010. Very-long-chain fatty acids are involved in polar auxin transport and developmental patterning in Arabidopsis. Plant Cell **22**, 364–375.

Růžička K, Šimášková M, Duclercq J, Petrášek J, Zažímalová E, Simon S, Friml J, Montagu MCEV, Benková E. 2009. Cytokinin regulates root meristem activity via modulation of the polar auxin transport. Proceedings of the National Academy of Sciences **106**, 4284–4289.

Salvi E, Rutten JP, Mambro RD, Polverari L, Licursi V, Negri R, Ioio RD, Sabatini S, Tusscher KT. 2020. A Self-Organized PLT/Auxin/ARR-B Network Controls the Dynamics of Root Zonation Development in Arabidopsis thaliana. Developmental Cell **53**, 431-443.e23.

Schaller GE, Bishopp A, Kieber JJ. 2015. The yin-yang of hormones: Cytokinin and auxin interactions in plant development. Plant Cell **27**, 44–63.

Scheres B, Krizek BA. 2018. Coordination of growth in root and shoot apices by AIL/PLT transcription factors. Current Opinion in Plant Biology **41**, 95–101.

Schindelin J, Arganda-Carreras I, Frise E, *et al.* 2012. Fiji: An open-source platform for biological-image analysis. Nature Methods **9**, 676–682.

Shang B, Xu C, Zhang X, Cao H, Xin W, Hu Y. 2016. Very-long-chain fatty acids restrict regeneration capacity by confining pericycle competence for callus formation in arabidopsis. Proceedings of the National Academy of Sciences of the United States of America **113**, 5101–5106.

Shimotohno A, Heidstra R, Blilou I, Scheres B. 2018. Root stem cell niche organizer specification by molecular convergence of PLETHORA and SCARECROW transcription factor modules. Genes & development **32**, 1085–1100.

Šimášková M, O'Brien JA, Khan M, *et al.* 2015. Cytokinin response factors regulate PIN-FORMED auxin transporters. Nature Communications **6**, 8717.

Thomas PD, Campbell MJ, Kejariwal A, Mi H, Karlak B, Daverman R, Diemer K, Muruganujan A, Narechania A. 2003. PANTHER: A library of protein families and subfamilies indexed by function. Genome Research **13**, 2129–2141.

Tian H, Jia Y, Niu T, Yu Q, Ding Z. 2014. The key players of the primary root growth and development also function in lateral roots in Arabidopsis. Plant Cell Reports **33**, 745–753.

Toyokura K, Goh T, Shinohara H, *et al.* 2019. Lateral Inhibition by a Peptide Hormone-Receptor Cascade during Arabidopsis Lateral Root Founder Cell Formation. Developmental cell **48**, 64-75.e5.

Trinh CD, Laplaze L, Guyomarc'h S. 2018. Lateral Root Formation: Building a Meristem de novo.

Annual Plant Reviews online.

Trinh DC, Lavenus J, Goh T, *et al.* 2019. PUCHI regulates very long chain fatty acid biosynthesis during lateral root and callus formation. Proceedings of the National Academy of Sciences of the United States of America **116**, 14325–14330.

Voß U, Wilson MH, Kenobi K, *et al.* 2015. The circadian clock rephases during lateral root organ initiation in Arabidopsis thaliana. Nature Communications **6**.

von Wangenheim D, Fangerau J, Schmitz A, Smith RS, Leitte H, Stelzer EHK, Maizel A. 2016. Rules and Self-Organizing Properties of Post-embryonic Plant Organ Cell Division Patterns. Current Biology **26**, 439–449.

Xuan W, De Gernier H, Beeckman T. 2020. The dynamic nature and regulation of the root clock. Development (Cambridge) **147**.

Zürcher E, Tavor-Deslex D, Lituiev D, Enkerli K, Tarr PT, Müller B. 2013. A robust and sensitive synthetic sensor to monitor the transcriptional output of the cytokinin signaling network in planta. Plant Physiology **161**, 1066–1075.

Figure legends

Figure 1. Time-course transcriptomic analysis of LRP formation in Col-0 and *puchi-1* after root gravistimulation. (A) Schematic diagram of the experimental procedure for the RNAseq analysis. (B) Number of differentially expressed genes (DEGs) in *puchi-1* compared to Col-0 at No LR, 12h, 18h, 24h, 30h and 36h after gravistimulation. Genes with a fold-change of up to Log2: +/- 1; p*<0.05 selected. (C) Distribution of elementary Gene Ontologies (GO) among either, upregulated genes or downregulated genes in *puchi* was analysed using a PANTHER overrepresentation assay and Fisher test followed by a Bonferroni Correction (p*<0.05). The Heat map shows the GO terms fold enrichment (FE) of DEGs for each time point. (D) Heat map of selected gene patterns up- and down-regulated in *puchi-1* compared to Col-0 background during the formation of LRP. Log 2-fold change (FC) of expression in *puchi-1* compared to WT is given. Statistical analysis on three independent RNAseq replicates were performed using the DESeq2 package and Wald Test: p-value: p*<0.05; p**<0.02; p***<0.01. Colour code for the heatmaps in (C) and (D) are red for upregulated genes and blue for downregulated genes. Colour code for gene names in (D) indicates the module classification (Orange: module1, Morphogenetic phase and Purple: module 2, Meristematic phase) as described in Lavenus *et al*., 2015.

Figure 2. *PUCHI* loss of function results in distinct expression patterns of meristematic phase regulator *PLT* genes during LRP development. (A-F) and (G-L) Expression pattern of *promPLT1:PLT1-YFP* and *promPLT4:PLT4-YFP* (green) respectively in *puchi-1* and Col-0 LR primordia. Stars indicate earlier detected signal expression during LRP outgrowth. Percentages and numbers indicate the occurrence of the represented pattern over the total number of observations. Cell walls were stained using propidium iodide (magenta). Scale bar: 25 µm.

Figure 3. *PUCHI* loss of function impacts QC marker gene expression patterns during LRP formation. Confocal microscopy images of expression of QC reporters (A-H) *QC25::CFP* and (I-P) *promWOX5::nls:GFP* (green) in LRP in Col-0 and *puchi-1*. Stars indicate earlier detected signal expression during LRP outgrowth. Percentages and numbers indicate the occurrence of the

represented pattern over the total number of observations. Cell walls were stained using propidium iodide (magenta). Scale bar: 25 µm.

Figure 4. *PUCHI* loss of function alters auxin and cytokinin signal distribution in developing LRP. (A) Heat map of selected auxin transporter gene patterns upregulated in *puchi-1* compared to Col-0 background during LRP formation. Log 2-fold change (FC) of expression in *puchi-1* compared to WT is given. Statistical analysis on the three independent RNAseq replicates were performed using the DESeq2 package and Wald Test: *p*-value: p*<0.05; p**<0.02; p***<0.01. (B-G) *DR5::GFP* (green), (H-O) *promPIN1::PIN1:GFP* (green) and (P-U) *promTCSn::GFP* (green) expression during LR development. Percentages and numbers indicate the occurrence of the represented pattern over the total number of observations. (B-M) Cell walls were stained using propidium iodide (magenta). (N-U) (Inset) Signal intensity monitor. (blue) low intensity; (red) high intensity. Scale bar: 25 µm.

Fig. 5. *PUCHI*-dependent early repression of meristem establishment. (A) Hypothetical model showing the role of *PUCHI* at early stages of LRP formation, *PUCHI* acts as a key regulator of spatiotemporal distribution of auxin balance and represses specific meristematic module genes.

Fig. S1: **LRP phenotype of Col-0 and *puchi-1* LRP during the time-course transcriptomic analysis after gravistimulation (hpg).** (A) and (B) Brightfield images showing the LRP stages observed for each timepoint. Time points corresponds to phenotype of the LRP observed in the RNAseq samples. The percentages of occurrence for each LRP stages per time point are shown. (C) Distribution of LRP developmental stages after 18, 24, 30 hours post-gravistimulation (hpg) in Col-0 and *puchi-1* roots. Data are one biological replicate for Col-0 and two biological replicates for *puchi-1*. The number of observed seedlings is indicated (n=X).

Fig. S2. GO-terms enrichment during the time-course transcriptomic analysis of LR formation in *puchi-1* compared to Col-0 upon gravistimulation. (A) Distribution of Gene

Ontologies among DEGs in *puchi* was analysed using a PANTHER overrepresentation assay and Fisher test followed by a Bonferroni Correction (p*<0.05). The Heat map shows the GO terms fold enrichment of DEGs for each time point.

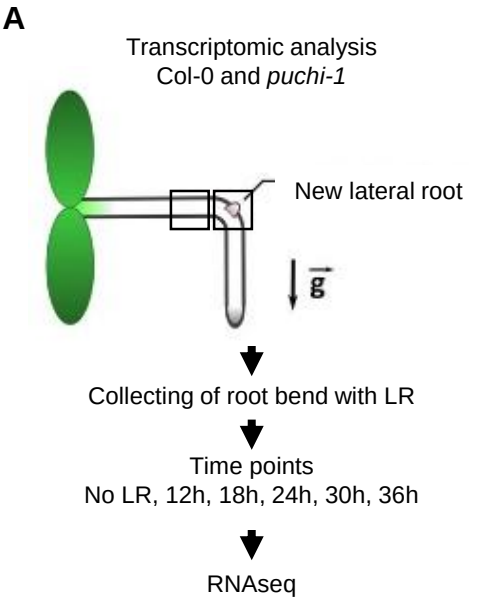
Figure S3. Time-course transcriptomic analysis in Col-0 and *puchi-1* after gravistimulation. Heat map of selected gene patterns up- and down-regulated in *puchi-1* compared to Col-0 background during the formation of LRP. Statistical analysis on three independent RNAseq replicates were performed using the DESeq2 package and Wald Test: p-value: *<0.05; **<0.02; ***<0.01. Colour code for the heatmap is red for upregulated genes and blue for downregulated genes. Colour code for gene names and AGI numbers indicates the module classification (Orange: module1, Morphogenetic phase and Purple: module 2, Meristematic phase) as described in Lavenus *et al*., 2015.

Fig. S4. Time-course transcriptomic analysis in Col-0 and *puchi-1* upon gravistimulation. (A) RT-qPCR analysis of *PLT1, PLT2*, *PLT3, PLT4*, *PLT5* and *PLT7* gene expression levels 24h after lateral root induction NPA/NAA treatment (Himanen *et al.,* 2002) in *puchi-1* and Col-0. Data are represented as mean ± SEM (standard error of the means), n=3 independent biological replicates. Significance was determined using a Student's t test (* $p< 0.05$, ** $p < 0.01$, *** $p < 0.001$). Expression pattern of (B-G) *promPLT2:PLT2-YFP* and (H-M) *promPLT3:PLT3-YFP* (green) in *puchi-1* and Col-0 LR primordia. Percentages and numbers indicate the occurrence of the represented pattern over the total number of observations. (B-M) Cell membranes were stained using propidium iodide (magenta). Scale bar: 25 µm.

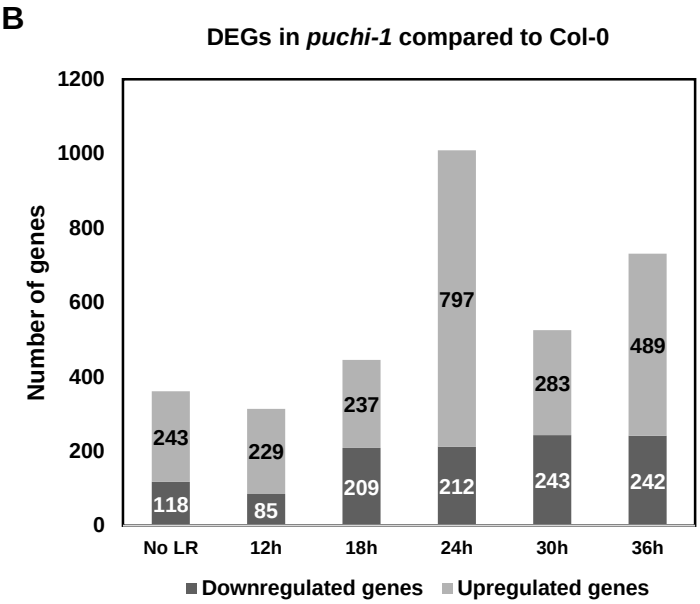
Figure S5. Identified PUCHI target genes in different datasets. (A) Venn diagram showing the number of targeted genes by PUCHI using DAPseq (Ronan *et al*., 2016; http://neomorph.salk.edu/dap_web/pages/index.php), RNAseq analysis in *puchi-1* background after gravistimulation (This paper) and PUCHI-GR inducible system (Trinh *et al*., 2019). Genes in pPUCHI::PUCHI:GR in *puchi-1* seedlings showed an upregulation (fold change ≥ 1.5, p-value

737 ≤0.05 as determined by Welch two sample t-test) in the following conditions were used: NAA CHX
738 DEX vs NAA CHX. (GR: GLUCOCORTICOID RECEPTOR; DEX: dexamethasone; CHX:
739 cycloheximide). (B) The common gene (red) between the three datasets and 25 genes (Auxin-;
740 cytokinin-; VLCFA-; LR-; meristematic- related and transcription factors) that were common
741 between two datasets (among a full list of 150 genes, Supp. Table 1) were selected and their AGI
742 number, aliases and TAIR summary are described in the table.
743
744 **Figure S6. Expression patterns of the 8 predicted PUCHI target genes.** (A-H) Gene expression
745 patterns in *puchi-1* and Col-0 background during the formation of LRP. Data are means +/- SE of
746 three replicates per time point from the transcriptomic dataset. Statistical analysis on RNAseq
747 replicates were performed using DESeq2 package and Wald Test: p-value: *<0.05; **<0.02;
748 ***<0.01.
749
750 **Fig. S7**: **Selected gene expression analysis in Col-0 and *puchi-1* after gravistimulation. (A-H)**
751 Gene expression patterns in *puchi-1* and Col-0 background during the formation of LRP. Data are
752 means +/- SE of three replicates per time point from the transcriptomic dataset. Statistical analysis
753 on RNAseq replicates were performed using DESeq2 package and Wald Test: p-value: *<0.05;
754 **<0.02; ***<0.01.
755
756

A



B



C

FE: 0 – 50 (GO biological process in *puchi-1* Downregulated genes); 0 – 10 (GO biological process in *puchi-1* Upregulated genes)

GO biological process in *puchi-1* Downregulated genes	No LR	12h	18h	24h	30h	36h
wax biosynthetic process (GO:0010025)	0	0	36	0	27	23
cuticle development (GO:0042335)	43	0	41	13	37	22
suberin biosynthetic process (GO:0010345)	0	48	46	0	0	0
cutin biosynthetic process (GO:0010143)	0	49	0	0	0	25
very long-chain fatty acid metabolic process (GO:0000038)	0	0	25	0	19	13
lipid transport (GO:0006869)	9	0	15	5	10	7
anther development (GO:0048653)	0	14	13	0	14	0

GO biological process in *puchi-1* Upregulated genes	No LR	12h	18h	24h	30h	36h
root development (GO:0048364)	0	0	0	5	0	0
anatomical structure morphogenesis (GO:0009653)	0	0	0	4	0	0
response to hormone (GO:0009725)	0	0	0	4	0	0
response to auxin (GO:0009733)	0	0	0	0	0	6

D

Log2 (FC): -6 – 3

	Gene Name	AGI Number	Log2 FC 12h	Log2 FC 18h	Log2 FC 24h	Log2 FC 30h	p-value 12h	p-value 18h	p-value 24h	p-value 30h
VLCFA	*KCS1*	AT1G01120	-0.37	-0.50	-0.15	-0.21	***	***	5E-01	2E-01
	KCS2	AT1G04220	-0.69	-0.69	-0.43	-0.21	***	***	*	2E-01
	KCS6	AT1G68530	-2.31	-1.85	-1.28	-4.04	***	***	***	***
	KCS8	AT2G15090	-5.70	-4.92	-5.64	-5.98	***	***	***	***
	KCS20	AT5G43760	-0.69	-0.50	-0.32	-0.15	***	**	2E-01	3E-01
	KCR1	AT1G67730	-0.64	-0.70	-0.03	-0.32	***	***	8E-01	***
	ECR	AT3G55360	-0.56	-0.56	0.02	-0.31	***	***	9E-01	***
	PAS2	AT5G10480	-0.33	-0.40	0.14	-0.08	*	*	3E-01	4E-01
Cutin/ Suberin	*GPAT8*	AT4G00400	0.00	-0.88	-1.81	-1.05	***	***	3E-01	**
	DCR	AT5G23940	0.07	-0.85	-2.11	-2.25	1E+00	***	***	***
	BDG	AT1G64670	-0.31	-3.52	-5.61	-4.00	8E-01	*	***	***
	GPAT4	AT1G01610	-0.85	-0.74	-0.20	-0.29	8E-01	***	***	***
Meristem establishment	*PLT1*	AT3G20840	1.01	2.11	1.89	1.36	**	***	***	***
	PLT4/BBM	AT5G17430	0.40	1.84	1.65	0.92	5E-01	***	***	***
	PLT2	AT1G51190	0.01	1.03	0.03	-0.78	1E+00	***	9E-01	***
	PLT3	AT5G10510	0.10	0.47	-0.02	-0.11	6E-01	***	9E-01	4E-01
	PLT5	AT5G57390	-0.81	-0.82	-1.43	-1.46	***	***	***	***
	PLT7	AT5G65510	0.37	-0.03	-0.87	-0.74	3E-01	9E-01	***	*

Figure 1. Time-course transcriptomic analysis of LRP formation in Col-0 and *puchi-1* after root gravistimulation. (A) Schematic diagram of the experimental procedure for the RNAseq analysis. (B) Number of differentially expressed genes (DEGs) in *puchi-1* compared to Col-0 at No LR, 12h, 18h, 24h, 30h and 36h after gravistimulation. Genes with a fold-change of up to Log2: +/-1; p*<0.05 selected. (C) Distribution of elementary Gene Ontologies (GO) among either, upregulated genes or downregulated genes in *puchi* was analysed using a PANTHER overrepresentation assay and Fisher test followed by a Bonferroni Correction (p*<0.05). The Heat map shows the GO terms fold enrichment (FE) of DEGs for each time point. (D) Heat map of selected gene patterns up- and down-regulated in *puchi-1* compared to Col-0 background during the formation of LRP. Log 2-fold change (FC) of expression in *puchi-1* compared to WT is given. Statistical analysis on three independent RNAseq replicates were performed using the DESeq2 package and Wald Test: p-value: p*<0.05; p**<0.02; p***<0.01. Colour code for the heatmaps in (C) and (D) are red for upregulated genes and blue for downregulated genes. Colour code for gene names in (D) indicates the module classification (Orange: module1, Morphogenetic phase and Purple: module 2, Meristematic phase) as described in Lavenus *et al*., 2015.

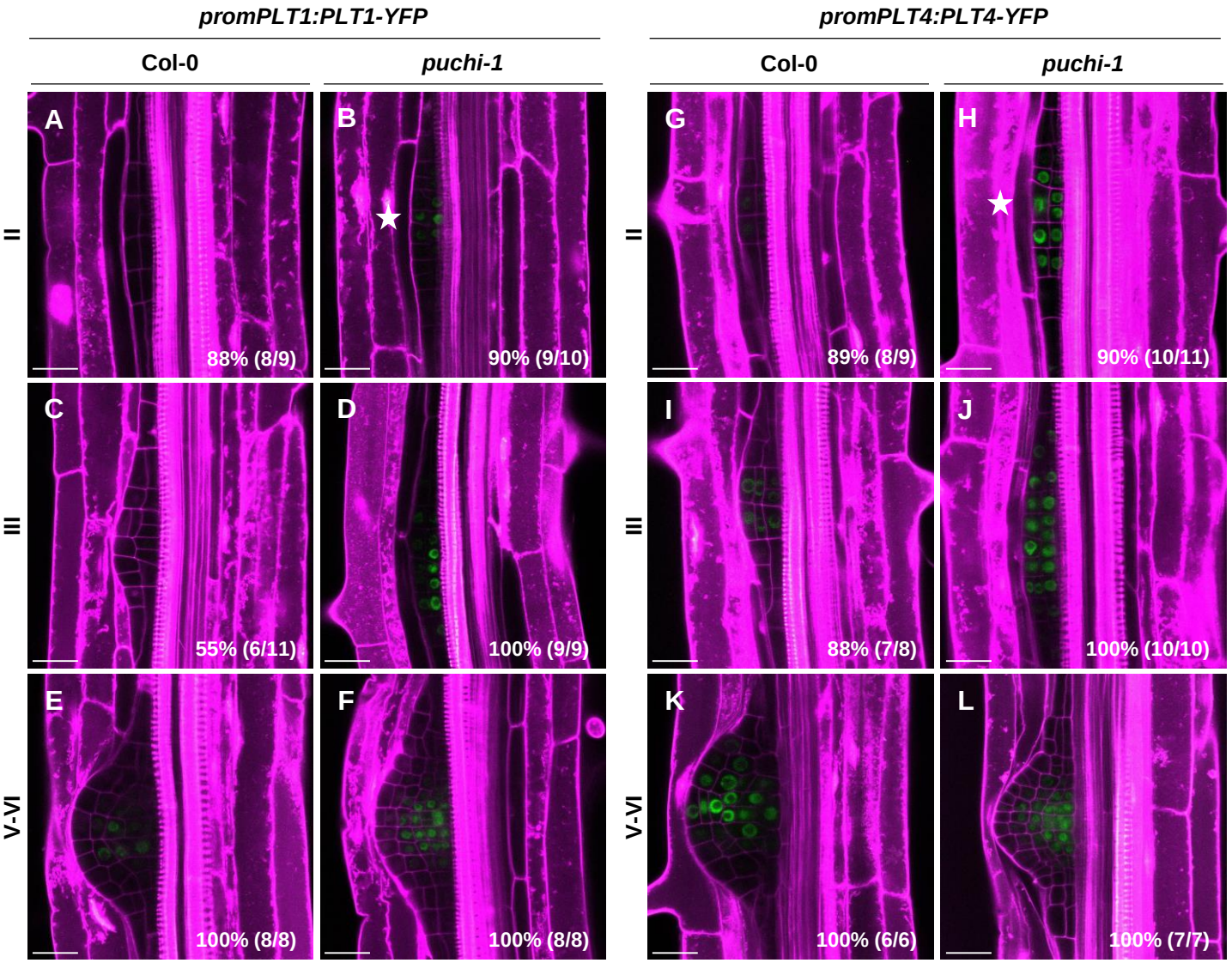


Figure 2. *PUCHI* loss of function results in distinct expression patterns of meristematic phase regulator *PLT* genes during LRP development. (A-F) and (G-L) Expression pattern of *promPLT1:PLT1-YFP* and *promPLT4:PLT4-YFP* (green) respectively in *puchi-1* and Col-0 LR primordia. Stars indicate earlier detected signal expression during LRP outgrowth. Percentages and numbers indicate the occurrence of the represented pattern over the total number of observations. Cell walls were stained using propidium iodide (magenta). Scale bar: 25 µm.

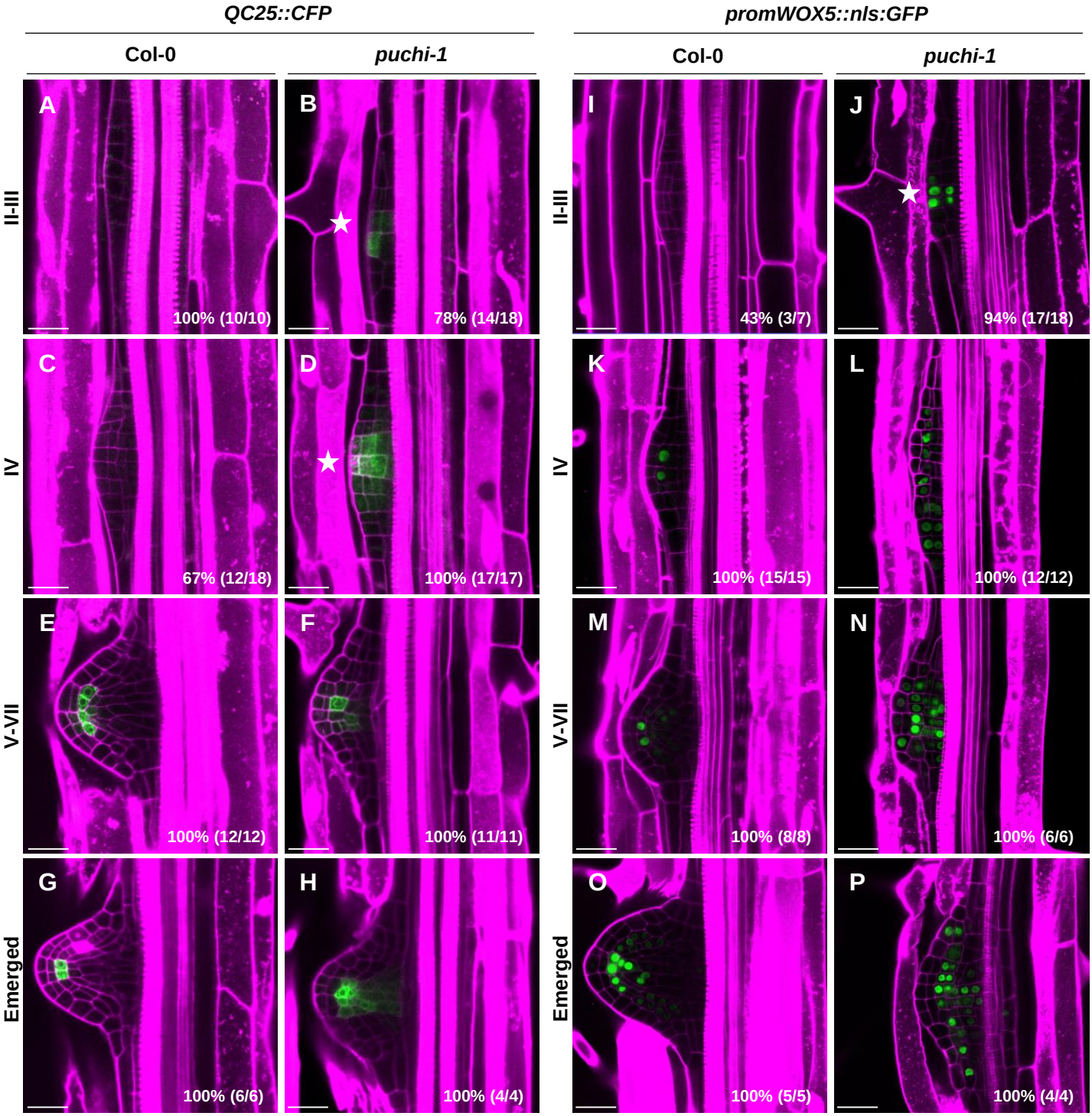
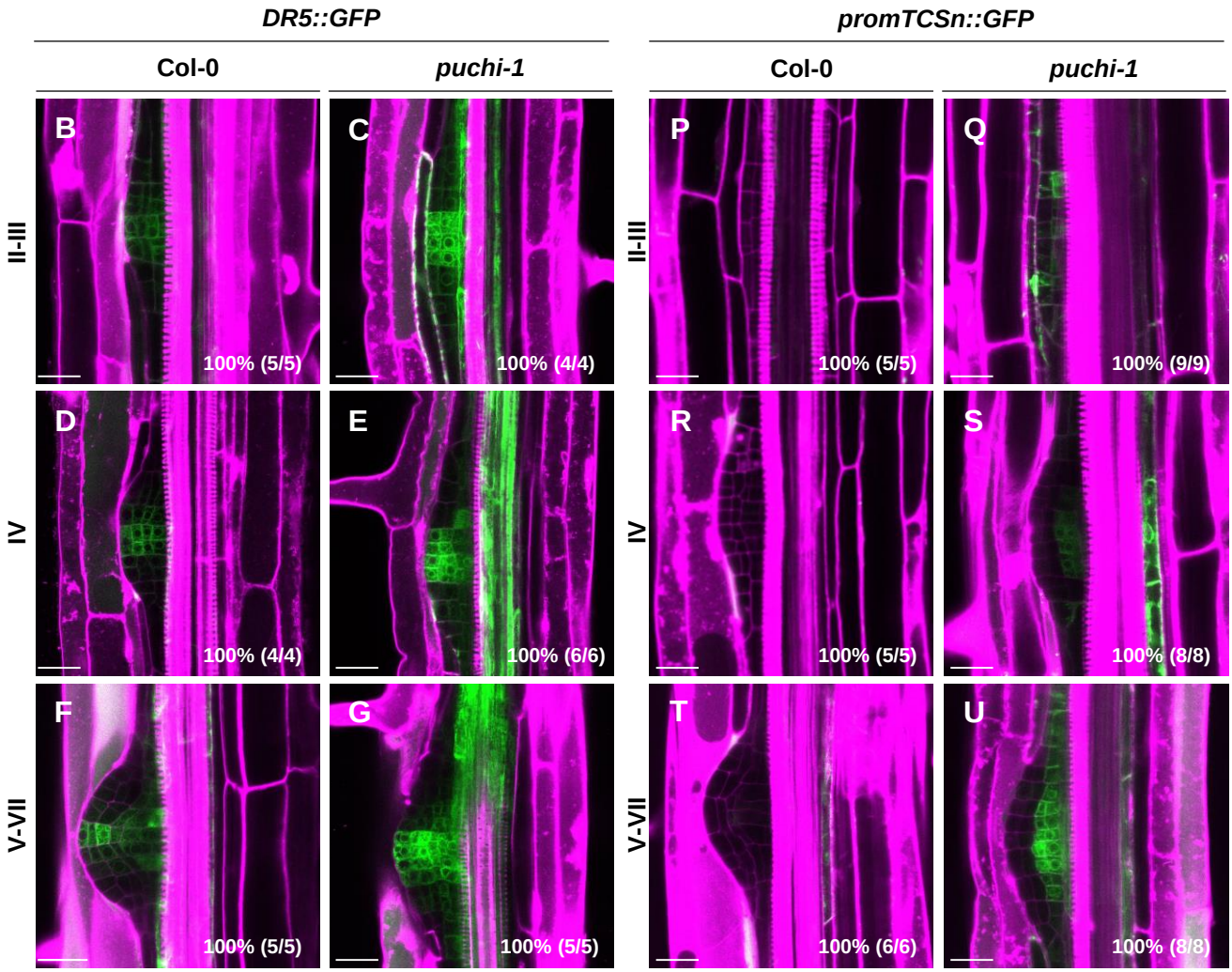


Figure 3. *PUCHI* loss of function impacts QC marker gene expression patterns during LRP formation. Confocal microscopy images of expression of QC reporters (A-H) *QC25::CFP* and (I-P) *promWOX5::nls:GFP* (green) in LRP in Col-0 and *puchi-1*. Stars indicate earlier detected signal expression during LRP outgrowth. Percentages and numbers indicate the occurrence of the represented pattern over the total number of observations. Cell walls were stained using propidium iodide (magenta). Scale bar: 25 µm.

A

Log2 (FC)
0 3

Gene Name	AGI Number	Log2 FC 12h	Log2 FC 18h	Log2 FC 24h	Log2 FC 30h	*p*-value 12h	*p*-value 18h	*p*-value 24h	*p*-value 30h
PIN1	AT1G73590	0.24	0.49	0.88	0.65	*	***	***	***
PIN4	AT2G01420	0.28	0.17	0.90	0.74	2.9E-01	3.9E-01	***	***
PIN7	AT1G23080	0.22	0.50	0.45	0.54	2.3E-01	***	***	***
PIN3	AT1G70940	0.47	0.59	0.75	0.67	***	***	***	***
LAX3	AT1G77690	0.44	0.42	0.71	0.63	**	***	***	***
IAA2	AT3G23030	0.21	0.41	0.34	0.76	1.7E-01	***	*	***
IAA29	AT4G32280	1.14	0.87	0.60	1.01	***	***	*	***



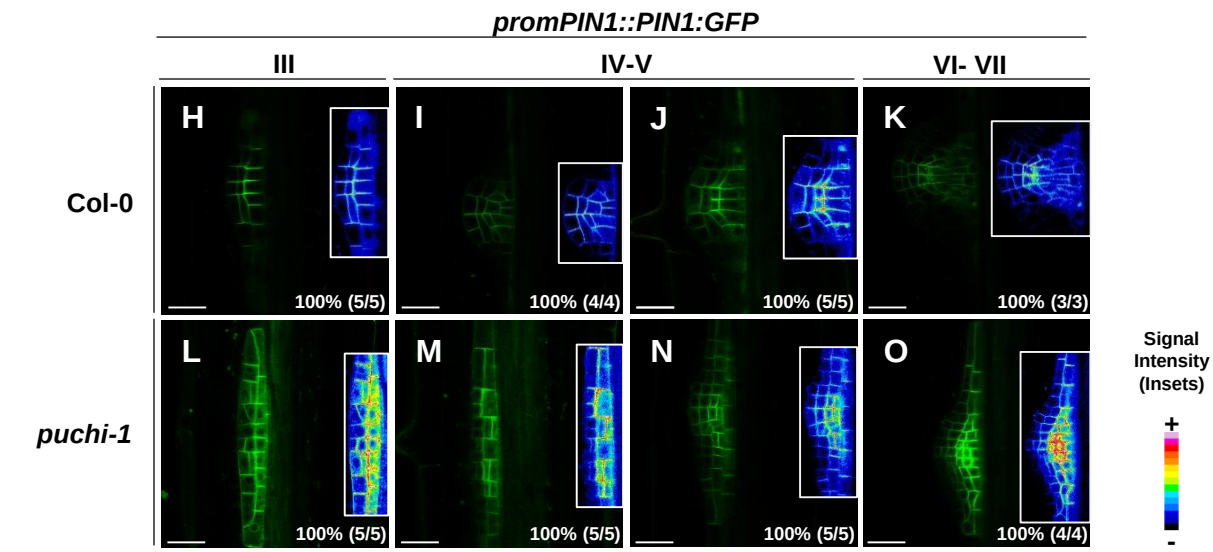


Figure 4. *PUCHI* loss of function alters auxin and cytokinin signal distribution in developing LRP. (A) Heat map of selected auxin transporter gene patterns upregulated in *puchi-1* compared to Col-0 background during LRP formation. Log 2-fold change (FC) of expression in *puchi-1* compared to WT is given. Statistical analysis on the three independent RNAseq replicates were performed using the DESeq2 package and Wald Test: *p*-value: p*<0.05; p**<0.02; p***<0.01. (B-G) *DR5::GFP* (green), (H-O) *promPIN1::PIN1:GFP* (green) and (P-U) *promTCSn::GFP* (green) expression during LR development. Percentages and numbers indicate the occurrence of the represented pattern over the total number of observations. (B-U) Cell walls were stained using propidium iodide (magenta). (H-O) (Inset) Signal intensity monitor. (blue) low intensity; (red) high intensity. Scale bar: 25 µm.

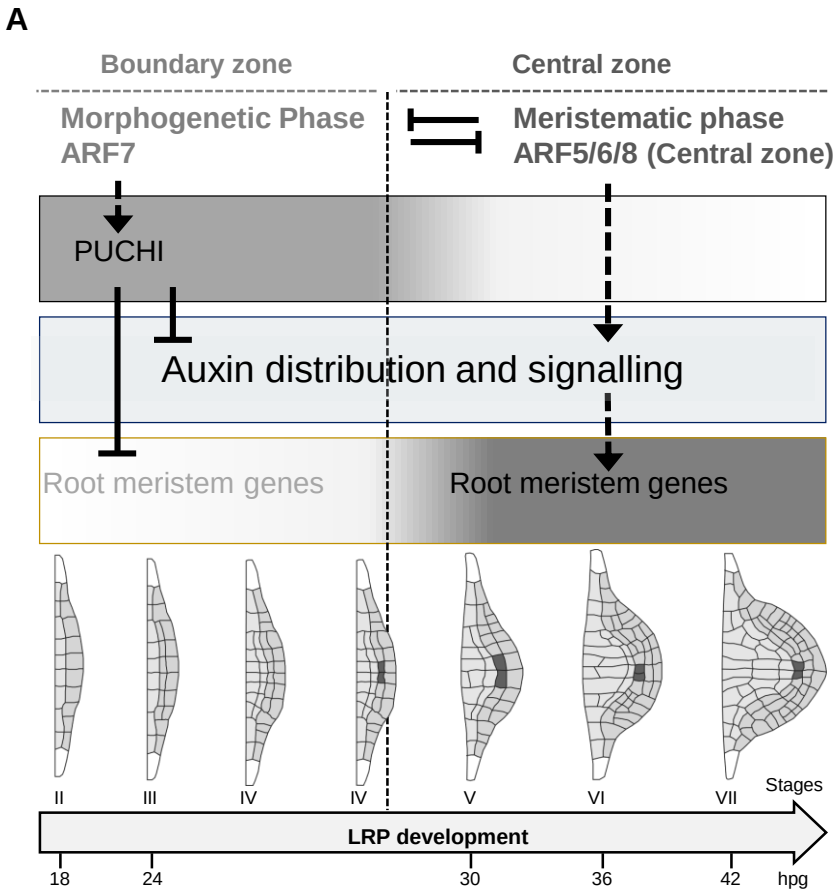
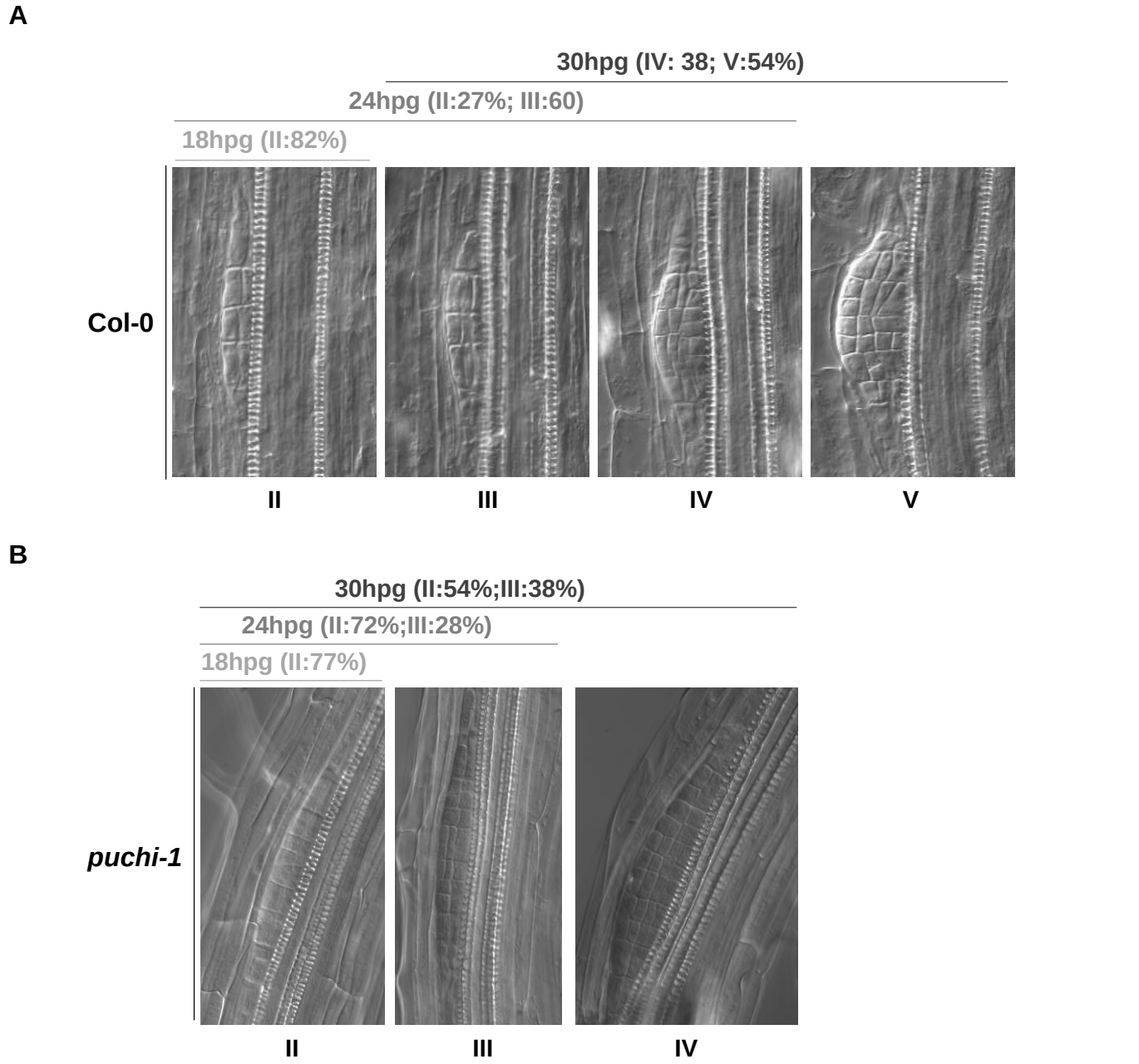


Fig. 5. *PUCHI*-dependent early repression of meristem establishment. (A) Hypothetical model showing the role of *PUCHI* at early stages of LRP formation, *PUCHI* acts as a key regulator of spatiotemporal distribution of auxin balance and represses specific meristematic module genes.



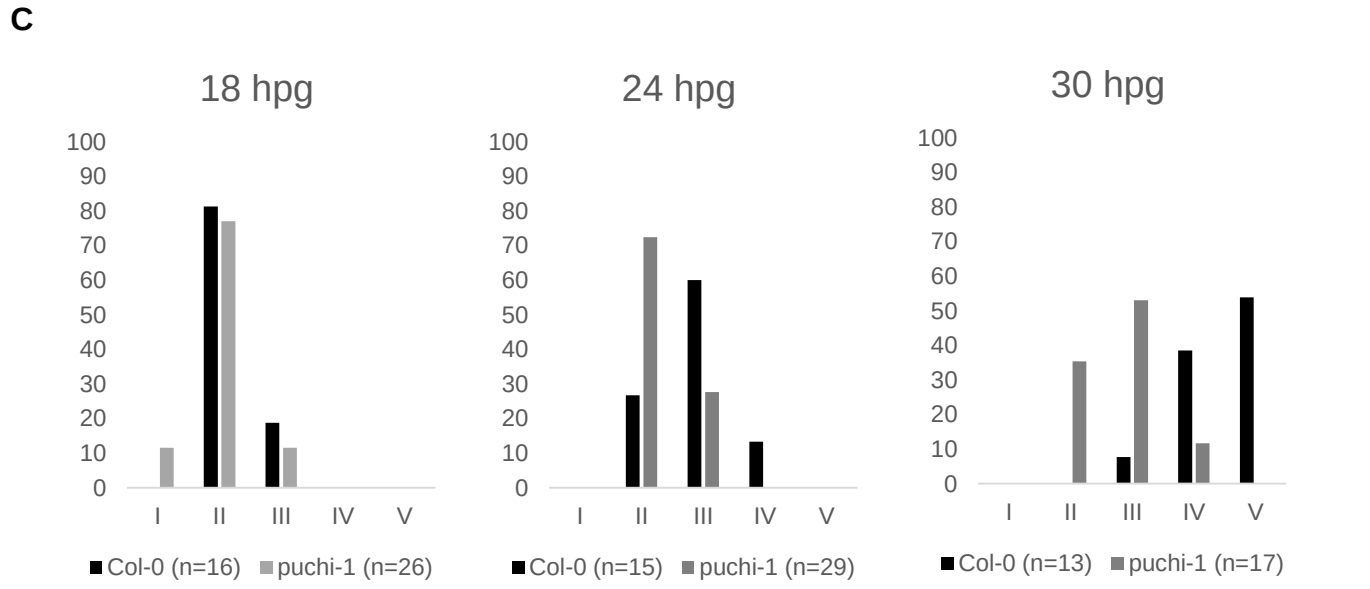


Fig. S1: **LRP phenotype of Col-0 and *puchi-1* LRP during the time-course transcriptomic analysis after gravistimulation (hpg).** (A) and (B) Brightfield images showing the LRP stages observed for each timepoint. Time points corresponds to phenotype of the LRP observed in the RNAseq samples. The percentages of occurrence for each LRP stages per time point are shown. (C) Distribution of LRP developmental stages after 18, 24, 30 hours post-gravistimulation (hpg) in Col-0 and *puchi-1* roots. Data are one biological replicate for Col-0 and two biological replicates for *puchi-1*. The number of observed seedlings is indicated (n=X).

A

GO biological process enrichment in *puchi-1* Downregulated genes						
	No LR	12h	18h	24h	30h	36h
wax biosynthetic process (GO:0010025)	0	0	36	0	27	23
cuticle development (GO:0042335)	43	0	41	13	37	22
suberin biosynthetic process (GO:0010345)	0	48	46	0	0	0
cutin biosynthetic process (GO:0010143)	0	49	0	0	0	25
fatty acid biosynthetic process (GO:0006633)	0	0	0	0	10	0
fatty acid metabolic process (GO:0006631)	0	9	0	0	0	0
very long-chain fatty acid metabolic process (GO:0000038)	0	0	25	0	19	13
lipid transport (GO:0006869)	9	0	15	5	10	7
response to fatty acid (GO:0070542)	0	0	0	5	0	0
lipid biosynthetic process (GO:0008610)	5	0	0	0	0	0
triterpenoid metabolic process (GO:0006722)	0	0	0	0	0	22
phyllome development (GO:0048827)	5	0	0	0	0	3
anther development (GO:0048653)	0	14	13	0	14	0
secondary metabolic process (GO:0019748)	0	0	0	5	0	0
response to stress (GO:0006950)	2	0	0	0	0	0
cellular response to hypoxia (GO:0071456)	0	0	0	8	0	0
response to salicylic acid (GO:0009751)	0	0	0	5	0	0
cell differentiation (GO:0030154)	0	0	0	0	0	3
GO biological process enrichment in *puchi-1* Upregulated genes						
	No LR	12h	18h	24h	30h	36h
root development (GO:0048364)	0	0	0	5	0	0
anatomical structure morphogenesis (GO:0009653)	0	0	0	4	0	0
cell growth (GO:0016049)	0	0	0	6	0	0
response to hormone (GO:0009725)	0	0	0	4	0	0
response to auxin (GO:0009733)	0	0	0	0	0	6
regulation of hormone levels (GO:0010817)	0	0	0	0	0	6
response to organic substance (GO:0010033)	4	0	0	0	0	0
response to wounding (GO:0009611)	0	0	0	0	7	0
cellular response to endogenous stimulus (GO:0071495)	0	0	0	5	0	0
response to jasmonic acid (GO:0009753)	0	0	0	0	9	0
response to fatty acid (GO:0070542)	0	0	0	0	9	0
regulation of transcription, DNA-templated (GO:0006355)	0	0	0	0	0	3

Fig. S2. GO-terms enrichment during the time-course transcriptomic analysis of LR formation in *puchi-1* compared to Col-0 upon gravistimulation. (A) Distribution of Gene Ontologies among DEGs in *puchi* was analysed using a PANTHER overrepresentation assay and Fisher test followed by a Bonferroni Correction (p*<0.05). The Heat map shows the GO terms fold enrichment of DEGs for each time point.

		Log2 FC						*p*-value					
Gene Name	**AGI Number**	**No LR**	**12h**	**18h**	**24h**	**30h**	**36h**	**No LR**	**12h**	**18h**	**24h**	**30h**	**36h**
QC specific													
NAP	AT1G69490	2,33	-0,06	1,08	0,14	2,98	2,02	***	9,4E-01	9,4E-02	7,9E-01	***	***
WIP4	AT3G20880	0,78	0,83	5,13	4,41	1,24	0,68	3,9E-01	5,6E-01	***	***	*	8,1E-02
DUF9	AT5G23780	0,48	0,36	1,10	0,48	0,61	0,14	3,7E-01	4,2E-01	***	1,1E-01	1,3E-01	6,4E-01
NPY4	AT2G23050	0,48	0,39	0,88	1,96	1,19	0,72	5,6E-01	6,1E-01	***	***	***	***
APL4	AT2G21590	-0,29	0,34	1,12	1,18	1,06	0,11	7,6E-01	5,4E-01	*	***	**	8,0E-01
WOX5	AT3G11260	0,10	0,55	0,64	-0,50	-0,75	-0,98	7,8E-01	1,1E-01	***	*	***	***
Morphogenesis													
FEZ	AT1G26870	0,18	0,39	-0,18	2,13	1,22	-0,70	8,6E-01	6,3E-01	8,0E-01	*	**	*
SHR	AT4G37650	0,14	0,06	0,31	0,46	0,33	0,36	5,3E-01	6,0E-01	***	***	***	***
SCR	AT3G54220	-0,07	0,06	-0,07	0,27	-0,06	-0,04	8,2E-01	6,5E-01	5,3E-01	6,4E-02	5,7E-01	7,3E-01
WER/MYB66	AT5G14750	-1,06	0,55	-0,17	0,65	-1,38	-2,44	4,3E-01	2,7E-01	6,2E-01	3,1E-01	***	***
MIR166b	AT3G61897	0,08	0,04	0,55	-0,18	-1,11	1,39	9,6E-01	9,7E-01	4,5E-01	8,4E-01	3,1E-01	7,4E-02
KAN4/ATS	AT5G42630	-1,27	0,10	-0,63	-0,98	-2,02	-1,64	**	7,6E-01	*	***	***	***
Auxin transport													
LAX3	AT1G77690	0,41	0,44	0,42	0,71	0,63	0,48	2,7E-01	**	***	***	***	***
Auxin signalling													
ARF2	AT5G62000	0,36	0,06	0,18	0,09	0,22	0,37	***	5,9E-01	1,6E-01	4,7E-01	**	***
MP/ARF5	AT1G19850	-0,13	-0,10	0,08	0,11	0,44	0,24	7,0E-01	6,7E-01	5,6E-01	3,2E-01	***	1,1E-01
ARF7	AT5G20730	-0,11	-0,07	-0,06	-0,02	-0,02	0,00	5,5E-01	5,6E-01	5,2E-01	7,6E-01	8,2E-01	9,9E-01
ARF9	AT4G23980	0,24	0,10	0,24	0,05	0,15	0,22	2,1E-01	3,2E-01	6,6E-02	6,3E-01	1,6E-01	6,8E-02
ARF11	AT2G46530	0,14	0,09	0,31	-0,07	0,20	0,18	6,2E-01	7,1E-01	2,1E-01	7,2E-01	3,4E-01	3,9E-01
ARF19	AT1G19220	0,13	0,14	0,17	0,35	0,17	0,27	4,8E-01	2,4E-01	8,9E-02	***	9,5E-02	*
ETT	AT2G33860	-0,03	0,08	0,05	-0,28	-0,28	-0,06	8,6E-01	5,7E-01	7,2E-01	4,3E-02	***	4,7E-01
ARF4	AT5G60450	-0,11	0,52	0,49	-0,02	0,24	0,10	3,8E-01	***	***	8,7E-01	*	4,2E-01
ARF6	AT1G30330	0,06	0,21	0,24	0,26	0,09	-0,07	8,7E-01	1,6E-01	*	*	3,8E-01	5,4E-01
ARF17	AT1G77850	0,16	0,25	0,24	-0,12	-0,06	0,05	3,7E-01	8,2E-02	8,1E-02	3,5E-01	7,3E-01	7,3E-01
IAA11	AT4G28640	0,09	0,14	0,22	0,25	0,43	0,58	7,5E-01	2,8E-01	1,9E-01	*	***	***
IAA13	AT2G33310	0,51	0,32	0,60	0,55	0,53	0,51	***	**	***	***	***	***
IAA2	AT3G23030	0,86	0,21	0,41	0,34	0,76	1,06	***	1,7E-01	***	*	***	***
IAA29	AT4G32280	1,21	1,14	0,87	0,60	1,01	1,71	1,0E-01	***	***	*	***	***
IAA5	AT1G15580	-0,32	0,84	1,04	1,33	0,53	1,06	6,3E-01	1,1E-01	8,7E-02	8,6E-02	3,4E-01	*
SLR/IAA14	AT4G14550	0,19	0,23	-0,01	0,50	0,32	-0,03	4,4E-01	1,0E-01	9,3E-01	***	*	8,9E-01
IAA19	AT3G15540	0,36	0,30	0,54	-0,17	0,25	0,12	5,1E-01	1,5E-01	***	1,2E-01	2,4E-01	5,4E-01
SHY2	AT1G04240	0,80	0,15	0,32	0,41	0,59	0,71	***	3,8E-01	6,2E-02	***	***	***
Auxin homeostasis													
GH3.1	AT2G14960	1,19	0,94	1,51	0,49	0,42	0,12	***	***	***	***	*	5,0E-01
YDK1/GH3.2	AT4G37390	1,53	0,47	0,77	0,55	0,59	1,17	***	*	***	1,1E-01	***	***
GH3.3	AT2G23170	2,32	0,61	0,88	1,09	1,60	2,08	***	4,0E-01	***	***	***	***
GH3.5	AT4G27260	1,24	0,85	1,17	0,87	0,80	1,09	***	***	***	***	***	***
DAO1	AT1G14130	0,13	-0,57	-0,87	-0,39	-0,36	-0,19	3,9E-01	***	***	**	***	1,3E-01
VLCFA and Cuticle													
CDEF1	AT4G30140	1,07	-0,71	0,43	0,20	0,49	1,19	4,6E-01	*	5,2E-01	8,2E-01	**	***
MPK14	AT4G36450	0,29	0,46	0,62	0,71	1,15	0,56	4,8E-01	1,8E-01	1,2E-01	*	*	2,1E-01
ERF13	AT2G44840	0,51	-0,57	-0,31	-1,81	0,92	0,12	3,3E-01	6,0E-01	8,3E-01	1,6E-01	1,6E-01	9,4E-01
Signalling													
GLV6	AT2G03830	-0,16	0,77	1,11	1,11	0,11	-0,72	8,5E-01	**	***	***	7,6E-01	***
MAKR4	AT2G39370	0,88	0,64	0,90	1,20	1,00	1,99	1,5E-01	***	***	***	***	***
MKK4	AT1G51660	-0,03	-0,27	-0,08	-0,52	-0,04	0,06	9,4E-01	2,3E-01	8,0E-01	*	8,0E-01	8,2E-01
MKK5	AT3G21220	-0,37	-0,19	-0,21	-0,34	-0,01	-0,31	7,6E-02	2,7E-01	1,4E-01	***	9,7E-01	***
MPK3	AT3G45640	0,32	-0,56	-0,25	-0,99	0,51	0,06	5,4E-01	3,7E-01	7,3E-01	***	8,9E-02	9,2E-01
TOLS2	AT4G37295	0,32	0,56	0,67	0,34	0,22	0,55	1,9E-01	**	***	*	1,5E-01	***
Transcription factors													
FLP/MYB124	AT1G14350	-0,65	-0,77	-0,68	-0,71	-0,39	-0,54	1,5E-01	***	***	***	4,3E-02	***
GATA23	AT5G26930	1,08	1,55	1,79	2,80	2,38	3,57	4,5E-01	***	***	***	***	***
LBD16	AT2G42430	-0,09	-0,93	-0,89	-1,11	-0,86	-0,44	8,3E-01	***	***	***	***	***
LBD18	AT2G45420	0,09	0,27	0,59	0,20	0,42	0,20	8,5E-01	1,5E-01	***	3,5E-01	*	4,8E-01
LBD29	AT3G58190	0,94	0,39	0,62	0,82	0,99	1,13	***	1,7E-01	***	***	***	***
Cytokinins													
CRF1	AT4G11140	-1,68	-2,64	-2,88	-2,40	-2,50	-2,24	***	***	***	***	***	***
CRF3	AT5G53290	0,09	0,58	0,71	0,54	0,65	0,38	7,0E-01	***	***	***	***	***
CRF2	AT4G23750	0,56	0,48	0,67	0,40	0,16	-0,18	1,9E-01	5,7E-02	***	***	2,5E-01	2,8E-01
CRF4	AT4G27950	-0,51	0,29	0,22	0,66	0,38	-0,21	2,4E-01	4,9E-01	4,2E-01	*	7,7E-02	5,4E-01
APT5	AT5G11160	-1,05	0,10	0,23	-0,14	-0,14	-0,52	1,4E-01	9,1E-01	6,3E-01	6,3E-01	6,1E-01	6,9E-02
AHP6	AT1G80100	-1,59	-1,24	-1,02	-0,87	-0,37	-1,56	*	5,6E-02	*	7,9E-02	4,5E-01	***
ARR5	AT3G48100	-0,73	-0,53	-0,12	0,10	0,02	-0,85	***	8,3E-02	3,7E-01	5,2E-01	9,5E-01	***
ARR14	AT2G01760	-0,04	-0,51	0,18	0,09	0,38	0,03	9,6E-01	3,0E-01	7,5E-01	8,0E-01	2,5E-01	8,9E-01
ARR18	AT5G58080	1,38	N/A	N/A	-0,46	-0,04	N/A	2,7E-01	N/A	N/A	7,1E-01	9,8E-01	N/A
ARR15	AT1G74890	-2,12	0,42	0,58	1,15	-0,99	-0,45		4,3E-01	2,1E-01	1,6E-02	1,9E-01	7,0E-01
ARR7	AT1G19050	-0,15	-0,07	-0,07	-0,13	-0,15	-0,67	8,6E-01	7,5E-01	7,2E-01	4,4E-01	4,4E-01	***
IPT7	AT3G23630	-0,60	-0,45	-0,50	-0,64	-0,56	-0,61	1,7E-01	*	***	***	***	**
IPT1	AT1G68460	-2,00	0,62	-1,47	0,40	-1,01	-2,40	2,4E-01	6,8E-01	2,3E-01	7,4E-01	4,4E-01	*
IPT3	AT3G63110	-0,62	0,06	-0,06	-0,34	-0,42	-0,27	6,7E-02	7,3E-01	7,0E-01	1,0E-01	**	2,7E-01
CKX1	AT2G41510	0,24	-0,24	0,01	0,89	0,82	1,31	6,8E-01	4,3E-01	9,6E-01	***	***	***
CKX6	AT3G63440	0,72	0,94	1,23	1,21	1,21	1,18	***	***	***	***	***	***
CKX5	AT1G75450	-0,71	0,12	0,16	-0,26	-0,09	-0,47	**	6,7E-01	2,5E-01	1,7E-01	7,1E-01	**
CKX2	AT2G19500	-0,37	N/A	N/A	N/A	-1,75	-1,77	8,7E-01	N/A	N/A	N/A	4,0E-01	1,2E-01
LOG3	AT2G37210	1,32	0,29	1,80	1,42	1,74	0,86	*	4,9E-01	***	***	***	***

Module 1 (Lavenus *et al*., 2015)
Module 2 (Lavenus *et al*., 2015)

Figure S3. Time-course transcriptomic analysis in Col-0 and *puchi-1* after gravistimulation. Heat map of selected gene patterns up- and down-regulated in *puchi-1* compared to Col-0 background during the formation of LRP. Statistical analysis on three independent RNAseq replicates were performed using the DESeq2 package and Wald Test: p-value: *<0.05; **<0.02; ***<0.01. Colour code for the heatmap is red for upregulated genes and blue for downregulated genes. Colour code for gene names and AGI numbers indicates the module classification (Orange: module1, Morphogenetic phase and Purple: module 2, Meristematic phase) as described in Lavenus *et al*., 2015.

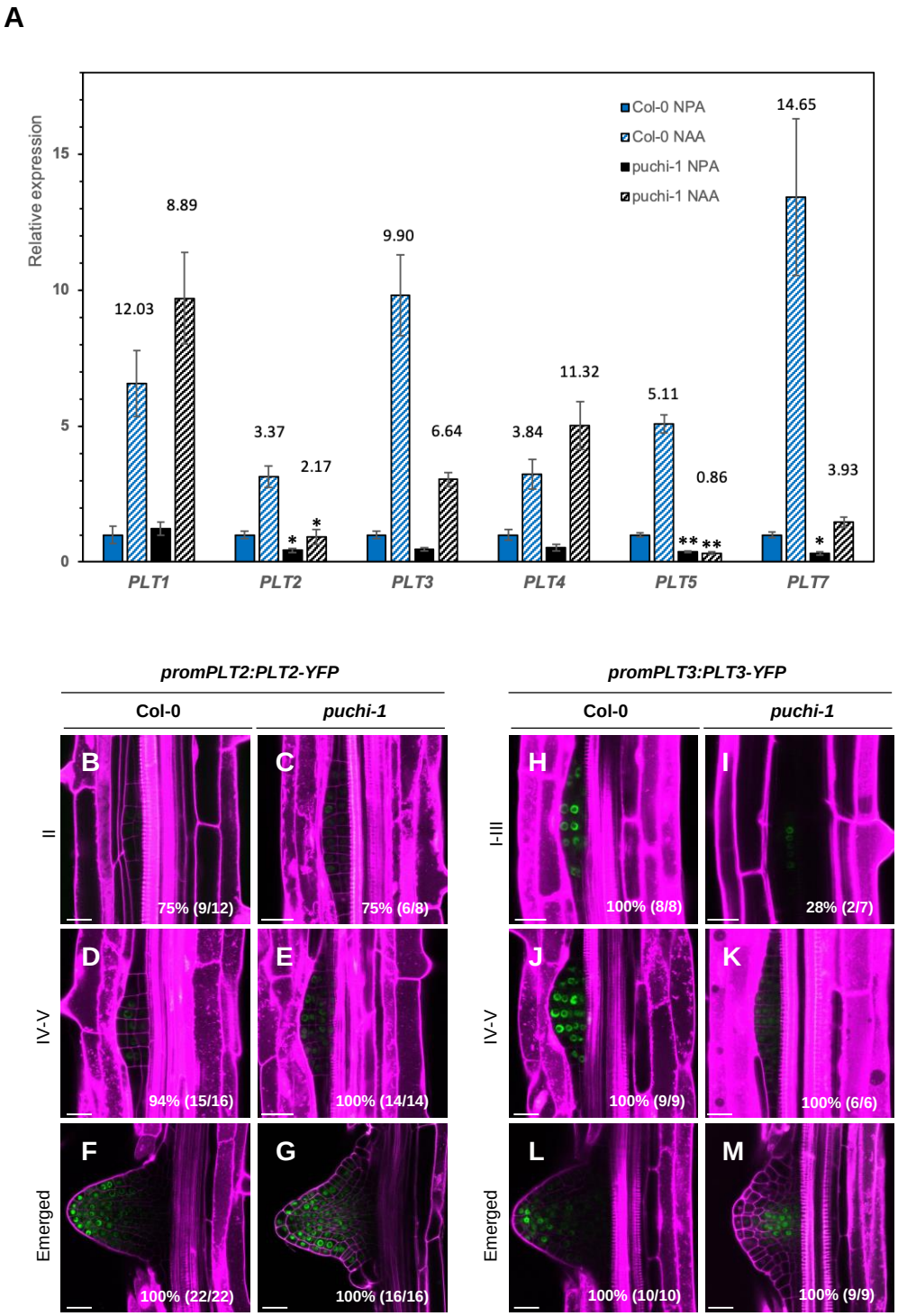
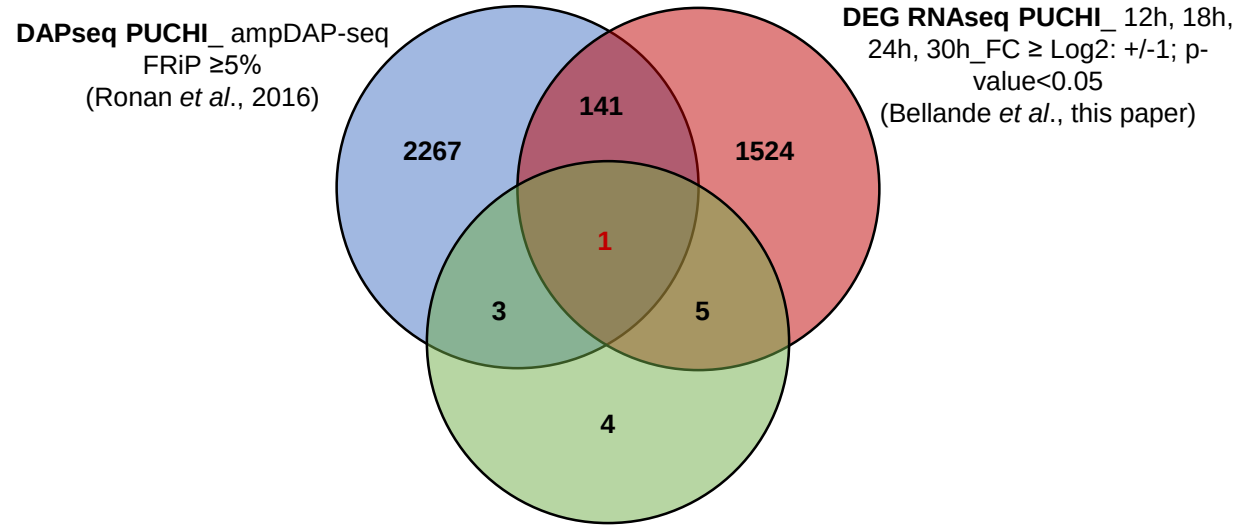


Fig. S4. Time-course transcriptomic analysis in Col-0 and *puchi-1* upon gravistimulation. (A) RT-qPCR analysis of *PLT1, PLT2*, *PLT3, PLT4*, *PLT5* and *PLT7* gene expression levels 24h after lateral root induction NPA/NAA treatment (Himanen *et al.,* 2002) in *puchi-1* and Col-0. Data are represented as mean ± SEM (standard error of the means), n=3 independent biological replicates. Significance was determined using a Student's t test (* $p < 0.05$, ** $p < 0.01$, *** $p < 0.001$). Expression pattern of (B-G) *promPLT2:PLT2-YFP* and (H-M) *promPLT3:PLT3-YFP* (green) in *puchi-1* and Col-0 LR primordia. Percentages and numbers indicate the occurrence of the represented pattern over the total number of observations. (B-M) Cell membranes were stained using propidium iodide (magenta). Scale bar: 25 µm.

A



B

AGI number	TAIR Aliases	TAIR Summary
AT4G11140	CRF1	Encodes a member of the ERF (ethylene response factor) subfamily B-5 of ERF/AP2 transcription factor family. The protein contains one AP2 domain. There are 7 members in this subfamily. CRF proteins relocalize to the nucleus in response to cytokinin.
AT3G51060	SRS1, STY1	A member of SHI gene family. Arabidopsis thaliana has ten members that encode proteins with a RING finger-like zinc finger motif. Despite being highly divergent in sequence, many of the SHI-related genes are partially redundant in function and synergistically promote gynoecium, stamen and leaf development in Arabidopsis. STY1/STY2 double mutants showed defective style, stigma as well as serrated leaves. Binds to the promoter of YUC4 and YUC8 (binding site ACTCTAC)
AT1G19790	SRS7	A member of SHI gene family. Arabidopsis thaliana has ten members that encode proteins with a RING finger-like zinc finger motif. Despite being highly divergent in sequence, many of the SHI-related genes are partially redundant in function and synergistically promote gynoecium, stamen and leaf development in Arabidopsis.
AT2G28500	LBD11	
AT3G56400	WRKY70	Member of WRKY Transcription Factor
AT4G29230	NAC075	NAC domain protein involved in negative regulation of flowering.
AT5G53950	ANAC098, CUC2	Transcriptional activator of the NAC gene family, with CUC1 redundantly required for embryonic apical meristem formation, cotyledon separation and expression of STM. Proper timing of CUC2 expression is required to maintain the phyllotactic pattern initiated in the meristem. CUC2 expression in leaf sinus region is required for serration and the extent of serration is modulated by mir164A mediated repression of CUC2. Together with CUC3-DA1-UBP15 part of a regulatory module which controls the initiation of axillary meristems, thereby determining plant architecture. Regulates the axillary meristem initiation, directly binding to the DA1 promoter.
AT1G28360	ERF12	encodes a member of the ERF (ethylene response factor) subfamily B-1 of ERF/AP2 transcription factor family (ERF12). The protein contains one AP2 domain. There are 15 members in this subfamily including ATERF-3, ATERF-4, ATERF-7, and leafy petiole. Regulates floral development.
AT1G12610	DDF1	Encodes a member of the DREB subfamily A-1 of ERF/AP2 transcription factor family (DDF1). The protein contains one AP2 domain. There are six members in this subfamily, including CBF1, CBF2, and CBF3. Overexpression of this gene results in delayed flowering and dwarfism, reduction of gibberellic acid biosynthesis, and increased tolerance to high levels of salt. This gene is expressed in all tissues examined, but most abundantly expressed in upper stems. Overexpression of this gene is also correlated with increased expression of GA biosynthetic genes and RD29A (a cold and drought responsive gene). Under salt stress it induces the expression of GAOX7, which encodes ad C20-GA inhibitor.
AT2G20880	ERF53	Encodes ERF53, a drought-induced transcription factor. Belongs to the AP2/ERF superfamily, and has a highly conserved AP2 domain. Regulates drought-responsive gene expressions by binding to the GCC box and/or dehydration-responsive element (DRE) in the promoter of downstream genes. Overexpression of AtERF53 driven by the CaMV35S promoter resulted in an unstable drought-tolerant phenotype in T2 transgenic plants. Involved in heat shock response.
AT5G24110	WRKY30	member of WRKY Transcription Factor
AT5G47220	ERF2	Encodes a member of the ERF (ethylene response factor) subfamily B-3 of ERF/AP2 transcription factor family (ATERF-2). The protein contains one AP2 domain. Functions as activator of GCC boxâ€"dependent transcription. Positive regulator of JA-responsive defense genes and resistance to F. oxysporum and enhances JA inhibition of root elongation.
AT1G29670	GDSL1	GDSL-motif esterase/acyltransferase/lipase. Enzyme group with broad substrate specificity that may catalyze acyltransfer or hydrolase reactions with lipid and non-lipid substrates. The mRNA is cell-to-cell mobile.
AT2G38110	GPAT6	bifunctional sn-glycerol-3-phosphate 2-O-acyltransferase/phosphatase. Involved in cutin assembly.
AT3G16370		GDSL-motif esterase/acyltransferase/lipase. Enzyme group with broad substrate specificity that may catalyze acyltransfer or hydrolase reactions with lipid and non-lipid substrates. The mRNA is cell-to-cell mobile.
AT5G56970	CKX3	It encodes a protein whose sequence is similar to cytokinin oxidase/dehydrogenase, which catalyzes the degradation of cytokinins.
AT4G26200	ACCS7, ACS7,	Member of a family of proteins in Arabidopsis that encode 1-Amino-cyclopropane-1-carboxylate synthase, an enzyme involved in ethylene biosynthesis. Not expressed in response to IAA.
AT1G51500	ABCG12, CER5	Encodes an ABC transporter involved in cuticular wax biosynthesis. Lines carrying recessive mutations in this locus have weakly glaucous stem surface, and relative elevated secondary alcohols and ketones.
AT1G43160	ERF113, RAP2.6	encodes a member of the ERF (ethylene response factor) subfamily B-4 of ERF/AP2 transcription factor family (RAP2.6). The protein contains one AP2 domain. There are 7 members in this subfamily.
AT5G57390	AIL5, PLT5	Encodes a member of the AP2 family of transcriptional regulators. May be involved in germination and seedling growth. Mutants are resistant to ABA analogs and are resistant to high nitrogen concentrations.essential for the developmental transition between the embryonic and vegetative phases in plants. Overexpression results in the formation of somatic embryos on cotyledons. It is also required to maintain high levels of PIN1 expression at the periphery of the meristem and modulate local auxin production in the central region of the SAM which underlies phyllotactic transitions. Acts redundantly with PLT3 and 7 in lateral root pattern formation.
AT2G14960	GH3.1	encodes a protein similar to IAA-amido synthases. Lines carrying an insertion in this gene are hypersensitive to auxin.
AT1G24470	KCR2	Encodes one of the two Arabidopsis homologues to YBR159w encoding a S. cerevisiae beta-ketoacyl reductase (KCR), which catalyzes the first reduction during VLCFA (very long chain fatty acids, >18 carbon) elongation: KCR1 (At1g67730), KCR2 (At1g24470). Complementation of the yeast ybr159Delta mutant demonstrated that the two KCR proteins are divergent and that only AtKCR1 can restore heterologous elongase activity similar to the native yeast KCR gene.
AT1G46264	HSFB4, SCZ	Encodes SCHIZORIZA, a member of Heat Shock Transcription Factor (Hsf) family. Functions as a nuclear factor regulating asymmetry of stem cell divisions.
AT1G71030	MYBL2	Encodes a putative myb family transcription factor. In contrast to most other myb-like proteins its myb domain consists of a single repeat. A proline-rich region potentially involved in transactivation is found in the C-terminal part of the protein. Its transcript accumulates mainly in leaves.
AT4G36260	SRS2, STY2	A member of SHI gene family. Arabidopsis thaliana has ten members that encode proteins with a RING finger-like zinc finger motif. Despite being highly divergent in sequence, many of the SHI-related genes are partially redundant in function and synergistically promote gynoecium, stamen and leaf development in Arabidopsis. Encodes protein with a single zinc finger motif and a members of a small gene family of putative transcription factors in which the SHORT INTERNODES (SHI) gene is found. STY2/STY1 double mutants showed defective style, stigma as well as serrated leaves.

Figure S5. Identified PUCHI target genes in different datasets. (A) Venn diagram showing the number of targeted genes by PUCHI using DAPseq (Ronan *et al.*, 2016; http://neomorph.salk.edu/dap_web/pages/index.php), RNAseq analysis in *puchi-1* background after gravistimulation (This paper) and PUCHI-GR inducible system (Trinh *et al.*, 2019). Genes in pPUCHI::PUCHI:GR in *puchi-1* seedlings showed an upregulation (fold change ≥ 1.5, p-value ≤0.05 as determined by Welch two sample t-test) in the following conditions: NAA CHX DEX vs NAA CHX. (GR: GLUCOCORTICOID RECEPTOR; DEX: dexamethasone; CHX: cycloheximide). (B) The common gene (red) between the three datasets and 25 genes (Auxin-; cytokinin-; VLCFA-; LR-; meristematic- related and transcription factors) that were common between two datasets (among the 150 genes, see suppl. Table 1 for detailis) were selected and their AGI number, aliases and TAIR summary are shown in the table.

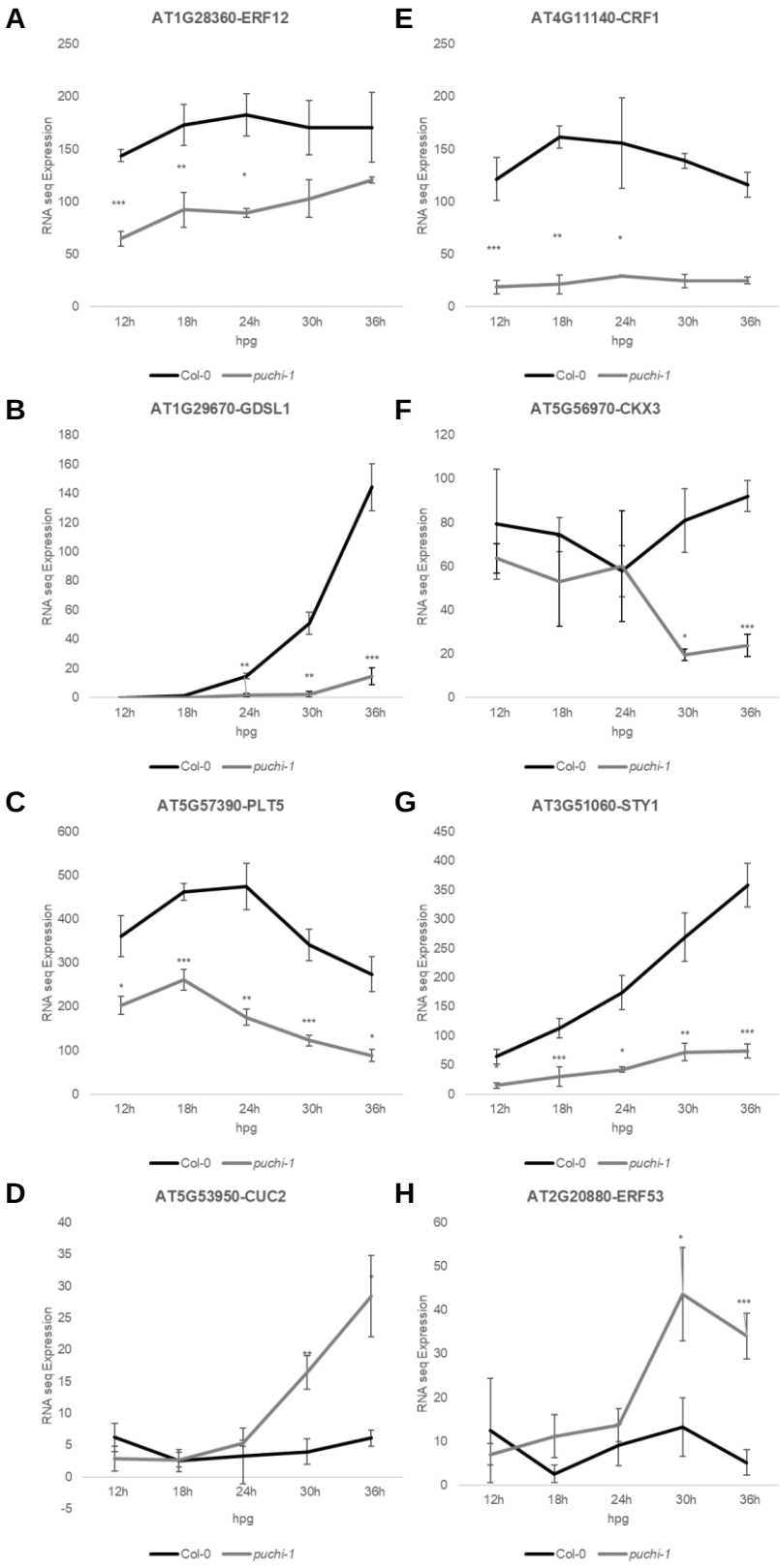


Figure S6. Expression patterns of the 8 predicted PUCHI target genes. (A-H) Gene expression patterns in *puchi-1* and Col-0 background during the formation of LRP. Data are means +/- SE of three replicates per time point from the transcriptomic dataset. Statistical analysis on RNAseq replicates were performed using DESeq2 package and Wald Test: p-value: *<0.05; **<0.02; ***<0.01.

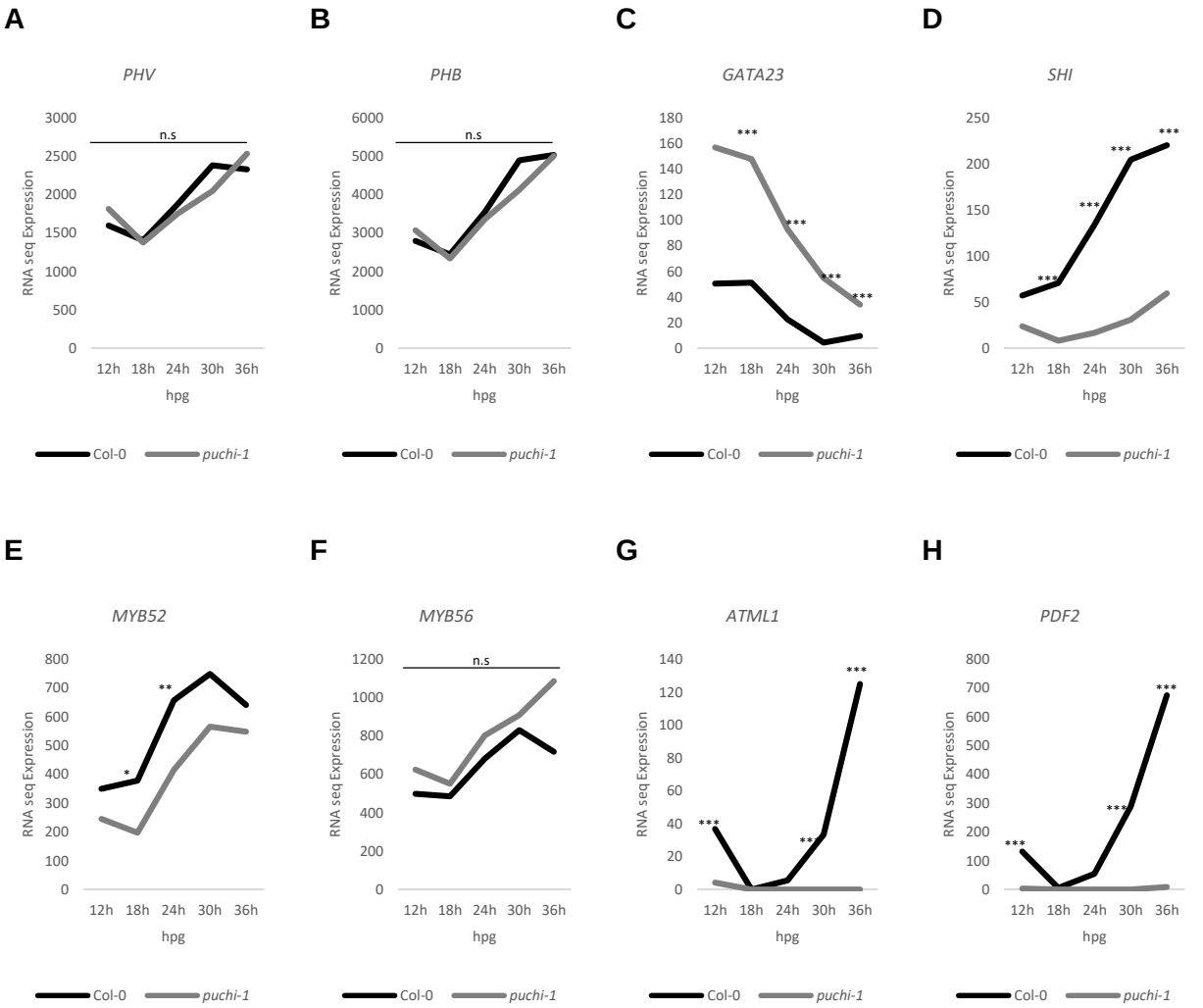


Fig. S7: **Selected gene expression analysis in Col-0 and *puchi-1* after gravistimulation. (A-H)** Gene expression patterns in *puchi-1* and Col-0 background during the formation of LRP. Data are means +/- SE of three replicates per time point from the transcriptomic dataset. Statistical analysis on RNAseq replicates were performed using DESeq2 package and Wald Test: p-value: *<0.05; **<0.02; ***<0.01.